الجمهورية الجزائرية الديمقراطية الشعبية
République Algérienne démocratique et populaire

وزارة التعليم العالي و البحث العلمي
Ministère de l'enseignement supérieur et de la recherche scientifique

جامعة سعد دحلب البليدة
Université SAAD DAHLAB de BLIDA

كلية التكنولوجيا
Faculté de Technologie

قسم الآلية والكهروتقني
Département d'automatique & Electrotechnique

Mémoire de Master

Filière Électrotechnique
Spécialité Machines électriques

Présenté par

Sadeddine Chamseddine

&

Ourari Roumaissa

Contribution to Optimal Power Flow in Radial Distribution Networks

Proposé par : Dr CHANANE Abdallah

Année Universitaire 2024-2025

Acknowledgements

First and foremost, I would like to express my heartfelt thanks to my family for their unconditional support throughout these long years of study. Their encouragement and belief in me have been a source of strength.
I extend my sincere gratitude to **Dr. CHANANE Abdallah** for his availability, guidance, and valuable advice during the development of this project. His contributions were truly appreciated during every step of this work.

I would also like to thank all the teachers and administrative staff at Saad Dahleb University and the Department of Electrical Engineering for their assistance and support throughout my academic journey.

It gives me great pleasure to dedicate this modest work to my beloved mother, my dear father, my sisters, all my friends, especially my friend **Amine Aissa**, and to everyone with whom I have shared wonderful moments.

Thank you all.

Sadeddine Chamseddine

In the name of Allah, the Most Gracious, the Most Merciful.
First and foremost, I thank Allah for granting me strength and guidance throughout my journey.

I express my deep gratitude to **Dr. Abdallah Chanane** for his continuous support and guidance during this project.

I also honor myself for the patience and determination that helped me achieve this accomplishment, and I pray for continued success in the future.

To the soul of my late father—may Allah have mercy on him—I hope I have made him proud.

My heartfelt thanks go to my beloved mother for her sacrifices, as well as to my aunt, who has been like a second mother to me, and to my sister and brothers.
And to my friends, especially my dear friend **Ghiatou Samira**, for her loyalty and unwavering support.

Ourari Roumaissa

ملخص : مع التعقيد المتزايد لشبكات التوزيع الحديثة، أصبحت الطرق التقليدية لحل مشكلة التدفق الأمثل للقدرة الكهربائية (OPF)غير فعّالة بشكل متزايد، وذلك بسبب محدوديتها في التعامل مع المتغيرات العديدة و دوال الهدف المعقدة. تقترح هذه المذكرة نهجًا من خطوتين لتحسين أداء شبكات التوزيع الكهربائي الشعاعية ومعالجة مشكلة التدفق الأمثل للقدرة الكهربائية. في الخطوة الأولى، يتم استخدام مؤشرات الحساسية للخسائر (LSIs) لتحديد العقد الأكثر أهمية في الشبكة. في الخطوة الثانية، يتم تطبيق خوارزميتين من خورزميات الادلة العليا ميتا هيوريستك—خوارزمية ذكاء السرب (PSO) وخوارزمية صقور هاريس—(HHO) لتحديد المواقع المثلى لتركيب المكثفات بهدف تعزيز أداء النظام. الهدف الرئيسي من هذا النهج هو تقليل التكلفة الكلية للنظام مع تحسين ملف الجهد وتقليل خسائر الطاقة. تم اختبار النهج المقترح والتحقق من فعاليته على نظام توزيع كهربائي شعاعي يتكون من 34 عقدة تابع لمعيار.IEEE

الكلمات المفتاحية: شبكات التوزيع الكهربائي الشعاعية، التدفق الأمثل للقدرة(OPF) ، مؤشر حساسية الخسائر(LSI) ، خوارزمية ذكاء
السرب(PSO) ، خوارزمية صقور هاريس(HHO) ، خوارزميات الادلة العليا الميتاهيورستيك، شبكة IEEE ذات 34 عقدة.

Résumé : Avec la complexité croissante des réseaux de distribution modernes, les méthodes traditionnelles de résolution du problème de l'écoulement de puissance optimal (OPF) deviennent de moins en moins efficaces, en raison de leurs limites face à la multiplicité des variables et à la complexité des fonctions objectif. Ce mémoire propose une approche d’optimisation en deux étapes pour traiter ce problème dans les réseaux de distribution radiaux. La première étape consiste à utiliser deux indices de sensibilité aux pertes (LSI) afin d’identifier les nœuds (bus) les plus critiques du réseau. La seconde étape applique deux algorithmes métaheuristiques — l’optimisation par essaim particulaire (PSO) et l’optimisation par faucons de Harris (HHO) — pour déterminer les emplacements optimaux des condensateurs et améliorer les performances du système. L’objectif principal est de minimiser le coût global du système tout en améliorant le profil de tension et en réduisant les pertes d’énergie électrique. L’approche proposée est testée et validée sur réseau de test radial IEEE 34-Bus.

Mots-clés : Réseau de distribution radial, l'écoulement de puissance optimal (OPF), Indice de sensibilité aux pertes (LSI), Optimisation par essaim particulaire (PSO), Optimisation par faucons de Harris (HHO), Algorithmes métaheuristiques, Placement optimal de condensateurs, Réseau de test IEEE à 34 nœuds.

Abstract: With the growing complexity of modern distribution networks, traditional methods for

solving the Optimal Power Flow (OPF) problem have become increasingly inadequate due to their limitations in handling multiple variables and complex objective functions. This thesis proposes a two-step optimization approach to address the OPF challenge in radial distribution systems. In the first step, Loss Sensitivity Indices (LSIs) are employed to identify the most critical buses in the network. In the second step, two metaheuristic algorithms—Particle Swarm Optimization (PSO) and Harris Hawks Optimization (HHO)—are applied to determine the optimal placement of capacitors for system enhancement. The primary objective is to minimize overall system cost while improving voltage profiles and reducing power losses. The proposed approach is tested and validated on the IEEE 34-bus radial distribution system.
Keywords: Radial Distribution Network, Optimal Power Flow (OPF), Loss Sensitivity Index (LSI), Particle Swarm Optimization (PSO), Harris Hawks Optimization (HHO), Metaheuristic Algorithms, Capacitor Placement, IEEE 34-Bus Test System.

List of Abbreviations and Acronyms:

Si: Apparent power at node *i*

PGi: Active power generated at node *i*

QGi: Reactive power generated at node *i*

Vi: Voltage at node *i*

δi: Voltage phase angle at node *i*

VS, IS: Voltage and current at the source

VR, IR: Voltage and current at the receiving end

Z: Line impedance

R, X: Line resistance and reactance

Y: Shunt admittance of the line

SDi: Apparent power demanded at bus *i*

PDi: Active power demanded at bus *i*

QDi: Reactive power demanded at bus *i*

gi: Conductance

bi: Susceptance

Pi: Active power injected at bus *i*

Qi: Reactive power injected at bus *i*

Vi, Vj: Voltage magnitudes at buses *i* and *j*

δi, δj: Voltage phase angles at buses *i* and *j*

Gij, Bij: Real and imaginary parts of the admittance matrix *Yij*

n: Total number of buses

X(t+1): Position of the hawk in the next iteration

X(t): Current position of the hawk

X_rabbit(t): Position of the prey

X_rand(t): Randomly chosen hawk's position

Xm(t): Average position of all hawks

LB, UB: Lower and upper bounds of the search space

r1 to r4, q: Random numbers in the interval (0, 1)

E: Current escaping energy of the prey

E0: Initial energy

t: Current iteration

T: Maximum number of iterations

HTB: High Voltage Category B

HTA: High Voltage Category A

BTB: Low Voltage Category B

BTA: Low Voltage Category A

TBT: Extra-Low Voltage Category

TSO: Transmission System Operator

PSO: Particle Swarm Optimization

HHO: Harris Hawks Optimization

AI: Artificial Intelligence

ML: Machine Learning

GA: Genetic Algorithms

ES: Evolution Strategies

DE: Differential Evolution

LSI: Loss Sensitivity Indices

BFS: Backward-Forward Sweep

KCL: Kirchhoff's Current Law

KVL: Kirchhoff's Voltage Law

Table of Contents

List of Figures

<u>Chapter 1:</u>

<u>Chapter 2:</u>

<u>Chapter 3:</u>

<u>Chapter 4:</u>

List of Tables

Chapter 4:

General Introduction

The reliable and efficient distribution of electrical energy is a cornerstone of modern civilization, enabling technological advancement, economic growth, and improved quality of life. Electrical distribution systems serve as the final stage in the delivery of electricity, linking high-voltage transmission networks to end users, ranging from households and small businesses to large industrial consumers. As the demand for electricity continues to rise due to urbanization, population growth, and the proliferation of electric devices, ensuring the efficiency and resilience of distribution networks has become more critical than ever.

Among the various distribution topologies, Radial Distribution Networks (RDNs) are the most widely used in urban and rural power systems due to their simplicity, low cost, and ease of operation. In an RDN, power flows in a single direction from the substation to the loads, following a tree-like structure. However, despite their advantages, RDNs suffer from several technical drawbacks, particularly under high load conditions or in large-scale systems. The most prominent challenges include significant voltage drops along feeders, high active and reactive power losses, poor voltage regulation, and limited fault tolerance. These issues can degrade power quality, increase operational costs, and even compromise the stability of the electrical system.

To address these limitations, Optimal Power Flow (OPF) strategies have been developed as essential tools to optimize the performance of power distribution systems. OPF techniques aim to minimize active power losses, maintain voltage profiles within acceptable limits, and achieve effective reactive power compensation—all while satisfying system constraints. Various methods have been employed to solve OPF problems, ranging from conventional mathematical programming to advanced artificial intelligence and metaheuristic approaches. Among these, metaheuristic algorithms have gained popularity due to their robustness, flexibility, and ability to handle complex, nonlinear, and multi-objective problems.

In this context, capacitor placement is one of the most practical and cost-effective techniques for reactive power compensation and loss reduction in RDNs. The optimal placement and sizing of capacitors can significantly enhance network efficiency. However, determining the best locations and sizes for these devices requires intelligent search strategies. This thesis proposes a two-stage optimization methodology tailored for radial distribution networks. In the first stage, Loss Sensitivity Indices (LSIs) are used to identify the most sensitive buses that would benefit from capacitor placement. In the second stage, two metaheuristic optimization techniques—Particle Swarm Optimization (PSO) and Harris Hawks Optimization (HHO)—are employed to determine the optimal capacitor sizes and locations, aiming to minimize active power losses, improve voltage profiles, and enhance overall system performance.

The proposed methodology is evaluated using the IEEE 34-bus radial test system. The effectiveness of PSO and HHO is compared in terms of power loss reduction, voltage regulation, and cost efficiency.

This thesis is organized into four chapters, each building progressively towards the development and evaluation of an efficient method for optimal capacitor placement in radial distribution networks.

Chapter 1 lays the theoretical foundation by presenting the fundamental concepts of electrical power systems, with a particular focus on distribution networks. It discusses different network topologies—radial, looped, and meshed—highlighting the advantages and limitations of each. The chapter also covers voltage levels across transmission and distribution systems, the hierarchical structure of power systems, and detailed modeling of key components such as lines, loads, and transformers. This foundational knowledge provides the necessary background for understanding the technical challenges addressed in the following chapters.

Chapter 2 focuses on the modeling and analysis of radial distribution networks, which are the primary subject of this study. It introduces the Backward-Forward Sweep (BFS) algorithm for power flow analysis, a method well-suited for the structure of RDNs due to its simplicity and efficiency. The chapter also introduces the Loss Sensitivity Index (LSI) technique, which is used to identify the buses most sensitive to power loss, making them ideal candidates for capacitor placement. The theoretical principles behind the LSI method, as well as the step-by-step process of its implementation, are discussed in detail to ensure clarity and reproducibility.

Chapter 3 is dedicated to metaheuristic optimization techniques, which are employed in the second stage of the proposed methodology. It begins by classifying the main types of metaheuristics (e.g., swarm-based, evolutionary, and nature-inspired) and discusses their relevance to power system optimization problems. The mechanisms, mathematical formulations, and operational logic of both Particle Swarm Optimization (PSO) and Harris Hawks Optimization (HHO) are explained in depth.

Chapter 4 presents the simulation results and discussion, based on the IEEE 34-bus radial test system. It details the performance of the two-stage optimization method, showing how the LSI-based preselection of candidate buses improves the efficiency of the overall search process. The results of PSO and HHO are then compared in terms of active power loss reduction, voltage profile improvement, and economic cost-effectiveness. While both methods demonstrated strong performance, HHO showed a consistently superior ability to balance the trade-offs between these objectives, making it the more effective algorithm in this context. The chapter concludes with a critical evaluation of the results.

By integrating sensitivity analysis with advanced metaheuristic optimization, this research contributes a systematic framework for improving the operational efficiency of Radial Distribution Networks, aligning with the evolving demands of modern power networks.

Chapter 1: Fundamentals of Electrical Networks

1.1 Introduction:

An electrical network is a set of energy infrastructures that enable the transmission of electrical energy from production centers to electricity consumers.

It consists of power lines operated at different voltage levels, interconnected through electrical substations.

Electrical substations distribute electricity and convert it from one voltage level to another using transformers.

For electrical energy to be usable, the transmission and distribution network must provide customers with the required power and ensure a stable voltage, with variations remaining within acceptable operational limits to maintain proper network functioning.

An electrical network must also ensure the dynamic management of the entire production–transmission–consumption system by implementing control mechanisms aimed at maintaining overall stability.

1.2 Topologies of Electrical Networks:

a) Meshed Network:

It is often used for network interconnections at the transmission and distribution levels. The meshed topology involves creating multiple loops or links between different interconnection substations using extra-high voltage (EHV) lines, forming a mesh structure.

❖ **Advantages:**

- High Reliability and Redundancy – The interconnected structure ensures that power can still be delivered even if one line fails, reducing the risk of outages.
- Load Sharing – Power flow can be distributed efficiently across multiple paths, preventing overloads on individual lines.

❖ **Disadvantages:**

- High Cost – Requires extensive infrastructure, including more transmission lines and substations, leading to higher investment and maintenance costs.
- Complex Management – The need for real-time monitoring and advanced control systems makes operation and coordination more challenging.

b) Looped Network:

This topology is mainly used in medium-voltage (MV) distribution and distribution networks. High-voltage (HV) or medium-voltage (MV) distribution substations, supplied from the extra-high voltage (EHV) network, are interconnected to form loops. The main purpose of this structure is to increase availability and reliability. However, it should be noted that MV networks are not necessarily looped.

❖ **Advantages:**

- Higher Availability and Reliability: If a failure occurs on one section of the loop, electricity can still be supplied from an alternative path, ensuring continuity of service.
- Load Balancing: The looped structure allows for better distribution of electrical loads, reducing congestion in certain parts of the network**.**

❖ **Disadvantages:**

- Higher Infrastructure Costs: More equipment, such as switches and circuit breakers, is required to manage the network, increasing costs.
- Complex Network Management: Requires advanced monitoring and control systems to regulate power flow and prevent overloads

c) Radial Network:

This is a simple topology commonly found in medium and low voltage distribution. It consists of a line powered by medium or low voltage distribution substations, which are initially supplied by a high or medium voltage source substation. In medium voltage, this structure is often powered from both ends to ensure availability and reduce the risk of power outages.

❖ **Advantages:**

- Simple and Cost-Effective: Easy to design, install, and maintain with lower infrastructure costs.
- Ease of Fault Detection: Since the network has a single path, faults are easier to locate.

❖ **Disadvantages:**

- Low Reliability: A single point of failure can lead to power outages since there's no alternative power path.

- Voltage Drop Issues: Since power flows in one direction, voltage drops can occur over long distances.

d) Tree Network:

This structure is widely used in rural areas and sometimes in urban areas where the load is not highly sensitive to interruptions. It consists of a distribution substation that supplies multiple distribution (low voltage) substations through branch connections at different levels of the medium-to-low voltage feeder lines.

❖ **Advantages:**

- Cost-Effective: Requires fewer transmission lines compared to meshed networks, reducing infrastructure costs.
- Efficient for Low-Density Areas: Well-suited for rural and low-load urban areas where high reliability is not a critical requirement.

❖ **Disadvantages:**

- Less Reliable: A fault in the main feeder can cut power to all connected branches, leading to widespread outages.
- Voltage Drop Issues: Power quality decreases with distance from the main substation, which can lead to inefficiencies.

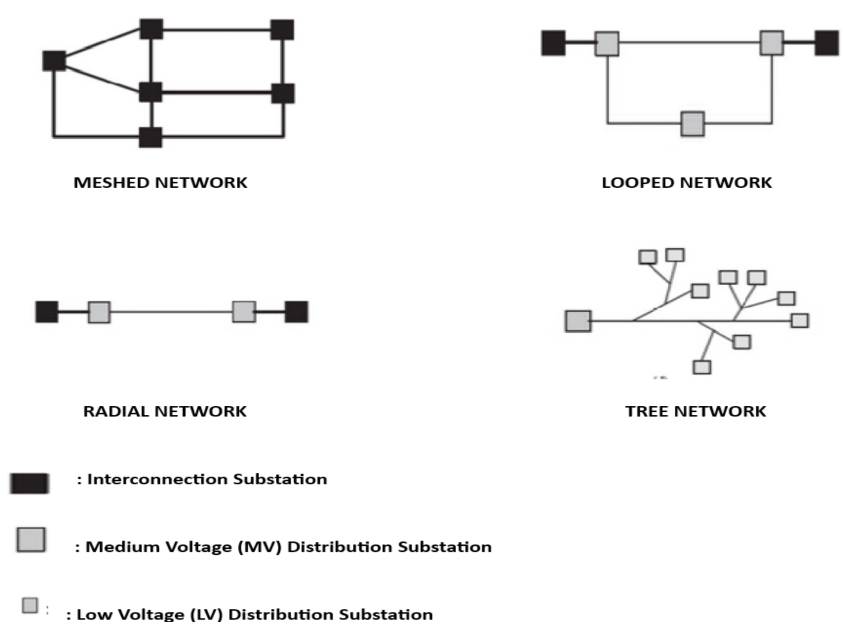

***Figure 1.1**: The Different Topologies of Electrical Networks*

1.3 Voltage Levels of Electrical Networks:

The new standard of the International Electrotechnical Commission (IEC), as well as the legislative texts in force in Algeria since June 2002, define the alternating voltage levels as follows (Figure 1.2) **[1]**:

- **HTB (High Voltage Category B)**: For a three-phase voltage exceeding 50 kV.
- **HTA (High Voltage Category A)**: three-phase voltage between 1 kV and 50 kV.
- **BTB (Low Voltage Category B)**: Three-phase voltage between 500 V and 1 kV.
- **BTA (Low Voltage Category A)**: Three-phase voltage between 50 V and 500 V.
- **TBT (Extra-Low Voltage Category)**: Equal to or less than 50 V.

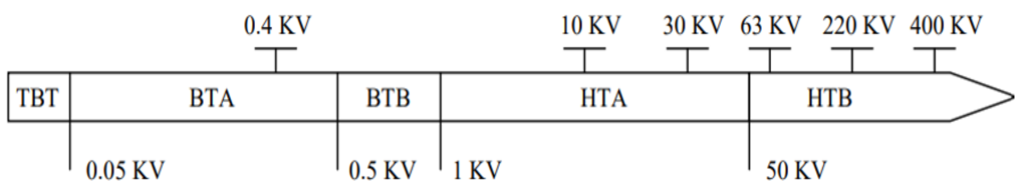

Figure 1.2: *Standardized Designations of the Different Voltage Levels*

1.4 Hierarchical Structure of Electrical Networks:

An electrical system is a set composed of production units, consumption units, electrical networks, and control centers. Its operation is managed by a Transmission System Operator (TSO).

The hierarchical structure of an electrical network varies in complexity depending on the voltage level, the power demand, and the required supply reliability. In general, electrical networks are divided into two main categories: Transmission/Sub-transmission networks and Distribution/Delivery networks **[2]**.

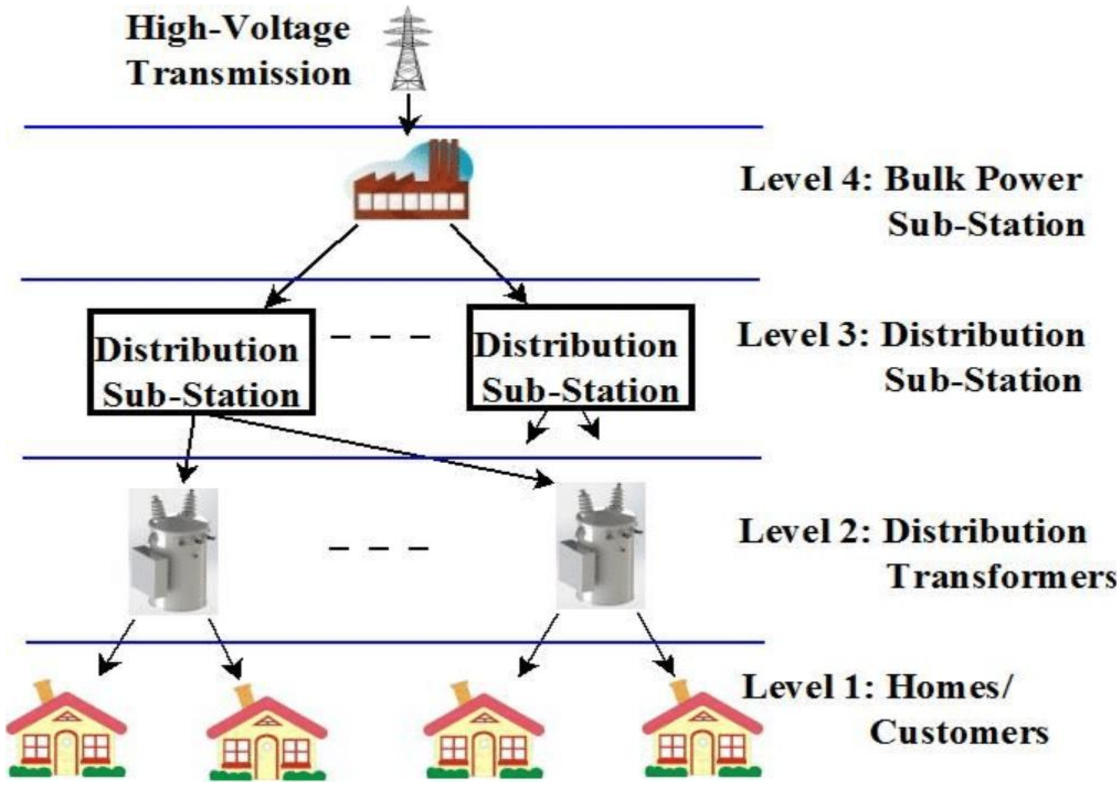

Figure 1.3: *Typical electricity distribution hierarchy*

a) Transmission Networks:

The transmission network consists of two types of lines: high-voltage (HTB) and medium-voltage (HTA) lines.

Transmission networks ensure the transportation of electrical energy over long distances. To minimize, among other things, Joule losses on the lines, these networks operate at very high voltage (from 63 kV to 400 kV) **[1, 2]**.

From a topographical perspective, for operational safety reasons, transmission networks are meshed or interconnected. This structure allows for:

- Collecting electricity produced by major power plants and transporting it in large volumes to consumption areas (transport function).
- Ensuring an economic and secure operation of production facilities by compensating for various contingencies (interconnection function).

The structure of these networks is mainly overhead. Their protection systems must be highly efficient, as these lines are crucial for the stability and security of the entire system. Power flows are distributed across all network lines, but their management is complex due to the high and variable power transfers between production and consumption zones. This complexity makes the techno-economic optimization of transmission networks challenging.

As a result, transmission networks are generally much more closely monitored than distribution networks. This supervision allows for voltage control, frequency regulation, power flow distribution, and production cost management, among other critical aspects.

b) Sub-Transmission Networks:

Sub-transmission networks, also known as High Voltage Networks, are responsible for distributing energy regionally from the transmission network. Their voltage levels exceed 60 kV, depending on the region **[1]**.

These networks primarily consist of overhead lines, each capable of transmitting more than 60 MVA over distances of several tens of kilometers.

Their structure is typically either a closed loop or, more commonly, an open loop. In some cases, they may also terminate in a radial (antenna) configuration at specific transformation substations **[1]**.

In densely populated urban areas, these networks must be underground, with cable lengths generally not exceeding a few kilometers.

Sub-transmission networks supply both:

- Distribution networks, through high-to-medium voltage (HT/MT) substations.
- Large industrial consumers (with loads exceeding 60 MVA), which require direct connection at this voltage level.

c) Distribution Networks:

The distribution network is the largest and most extensive part of the electrical system, ensuring local energy distribution. These networks operate at voltages equal to or below 50 kV (Medium Voltage – HTA) **[2]**.

They are classified into two types:

- Medium Voltage (MV) Networks (10 kV – 30 kV): Connected to the transmission network.
- Low Voltage (LV) Networks (0.4 kV): Representing the final stage of electrical distribution.

The LV network is the last link in the electrical system, with its sections connected to the MV network through medium-to-low voltage (HTA/BT) substations.

These voltage levels provide a techno-economic balance, which:

- Reduces voltage drops
- Minimizes the number of source substations (High-to-Medium Voltage, HTB/HTA)
- Limits technical and economic constraints associated with high-voltage infrastructure.

d) Delivery Networks:

This is the network we are most familiar with, as it operates at 400V/230V. The main purpose of this network is to deliver electricity from the distribution network to low-consumption points in public areas, granting access to subscribers. It represents the final stage in an electrical network structure **[1]**.

At this level, power is delivered using two different topologies, depending on the location of the loads:

- Urban Networks: Power is transmitted via underground cables. This type of network is characterized by a high load density, and its topology is divided into three categories: multi-branch networks, radial feeder networks, and highly meshed networks.

- Rural Networks: Power is transmitted via overhead lines. These networks are characterized by low load density and sparse meshing, with loops between source substations.

1.5 Representation and Analysis of Electrical Networks:

The complexity of electrical networks makes their representation and analysis using conventional diagrams impractical.

To simplify their representation and analysis, several tools have been developed, including the single-line diagram in which the interconnections of different equipment are indicated by a single line while actual electrical connections are not represented, phase analysis (using the equivalent single-phase circuit), and the per-unit (PU) system.

a) Single-line diagram (SLD):

The single-line diagram is only used to indicate all the details of the network. The network analysis is performed using the equivalent single-phase circuit. Finally, the actual three-phase values are derived from the single-phase values using the relationships of a balanced three-phase system.

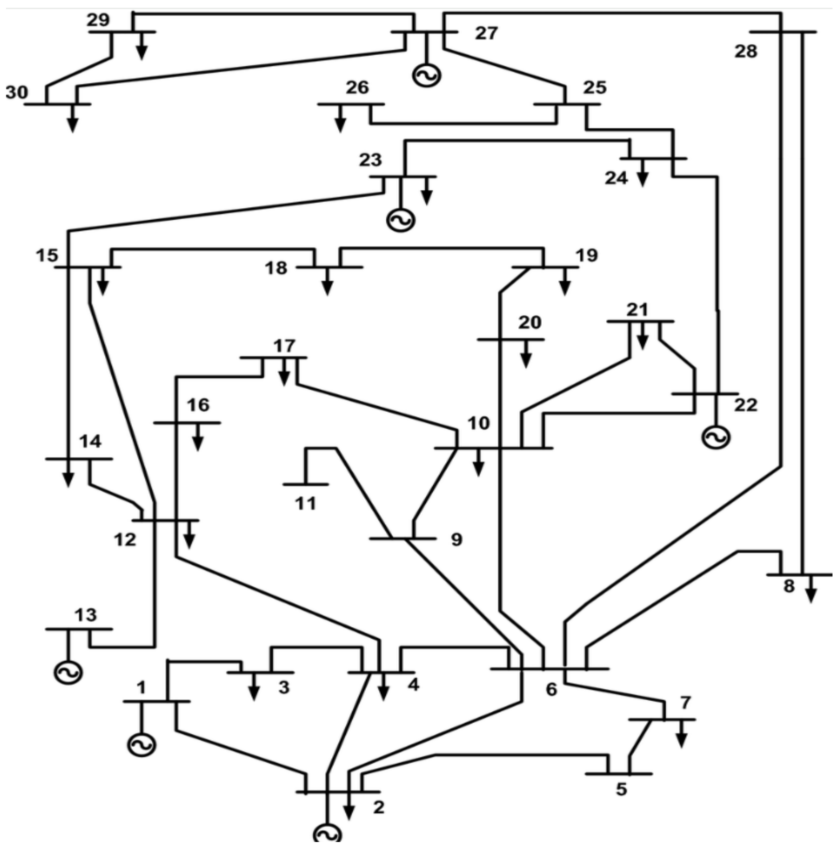

Figure 1.4: *Single-line diagram of IEEE 30 bus system*

b) Per-phase analysis or equivalent single-phase circuit:

The analysis of a balanced three-phase system can be simplified by transforming it into a Y system and considering only the equivalent single-phase circuit, which represents phase A alone.

The voltages and currents of the other phases are then derived from the voltages and currents of phase A by adding the phase shifts.

c) Per-unit system (PU system):

Power system analysis calculations can be simplified using the per-unit (PU) system. In this system, quantities such as voltage, current, impedance, and power are expressed relative to chosen base values. To use the per-unit system, two base values must first be selected. In most cases, a line-to-neutral base voltage ($VbaseLN$) and a base apparent power ($Sbase$) are chosen, from which other base values are derived:

- **Base current:**

$$\boldsymbol{I_{base} = \frac{S_{base}}{V_{baseLN}}}$$

- **Base impedance:**

$$\boldsymbol{Z_{base} = R_{base} = X_{base} = \frac{V_{baseLN}^2}{S_{base}}}$$

In the given electrical system, variables are expressed as unitless fractions of the base values:

$$\textbf{Per} - \textbf{unit value} = \frac{\textbf{Actual value}}{\textbf{Base value}}$$

Thus, calculations can be performed in per-unit values, and actual values are obtained by multiplying per-unit values by base values.

❖ **Advantages of the per-unit system are:**

- Numbers are smaller (typically around 1.0).
- It simplifies the comparison of different power system characteristics.
- eliminates the need for unit conversions when transitioning between voltage levels.
- facilitates power flow and short-circuit studies by using standardized system parameters.

1.6 Modeling of electrical network components:

In modern power systems, electrical networks are operated near their physical limits. Previously, when infrastructures were designed with significant safety margins, this was not a major concern. However, with increasing demand and constrained resources, accurate modeling has become essential to maintain network stability and prevent disruptions.

An electrical power network consists of several key components, including power generators, transmission and distribution lines, transformers, and electrical loads. Additionally, it incorporates protective devices and auxiliary equipment. Generally, the electrical system is divided into three primary subsystems:

- Generation (power production units)
- Transmission and distribution (network infrastructure and substations)
- Consumption (end users and electrical loads)

Due to the complexity of an electrical power network, its representation must be simplified to develop equivalent models or schematics for key components such as generators, various types of transformers, transmission lines, and loads. These models are then integrated into computational programs to simulate their effects on the entire system **[2]**.

a) Modeling of generators:

Generators play a crucial role in converting different forms of energy—such as mechanical, photonic, and chemical—into electrical energy. They are capable of supplying both active and reactive power while ensuring voltage regulation at a specified level. Essentially, a generator can be represented as a source of active and reactive power that maintains a predefined voltage setpoint **[3, 4]**.

However, the operation of a generator is subject to various constraints, including the thermal limits of the rotor and stator, as well as steady-state stability restrictions. These limitations affect the maximum active and reactive power that the generator can deliver. As a result, the generator can be modeled according to the schematic representation shown in figure 1.5 **[3, 4]**.

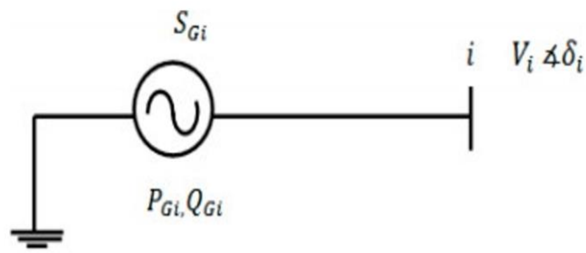

Figure 1.5: *Generator Model*

The following parameters define the generator model:

- $\boldsymbol{Si}$**:** Apparent power at node i
- $\boldsymbol{PGi}$**:** Active power generated at node i
- $\boldsymbol{QGi}$**:** Reactive power generated at node i
- $\boldsymbol{Vi}$**:** Voltage at node i
- $\boldsymbol{\delta i}$**:** Voltage phase angle at node i

b) Transmission lines:

A transmission line is generally modeled using an equivalent π circuit, which consists of a series impedance (resistance R in series with an inductive reactance X) and a shunt admittance that includes a capacitive susceptance B (due to the capacitive effect between the line and the ground) in parallel with an insulation conductance G **[2, 4]**.

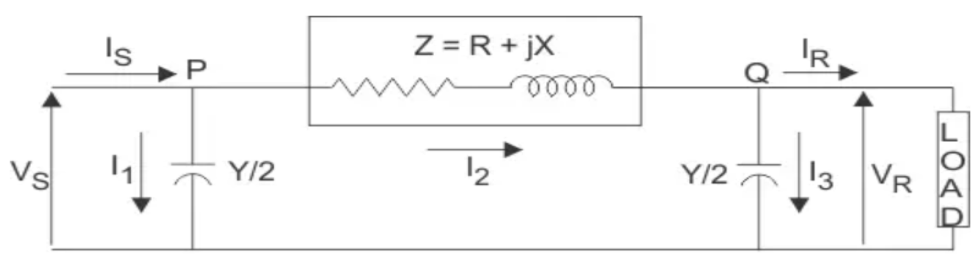

Figure 1.6: *π model of a transmission line*

- V_S, I_S: Voltage and current at the source, respectively.
- V_R, I_R: Voltage and current at the receiving end, respectively.
- Z: Line impedance.
- R, X: Line resistance and reactance, respectively.

- Y: Shunt admittance of the line.

Applying Kirchhoff's law to determine the voltage and current at the source, we obtain the following system of equations:

$$\begin{cases} V_s = A \cdot V_R + B \cdot I_R \\ I_s = C \cdot V_R + D \cdot I_R \end{cases} \tag{1.1}$$

In matrix form:

$$\begin{bmatrix} V_S \\ I_S \end{bmatrix} = \begin{bmatrix} A & B \\ C & D \end{bmatrix} \begin{bmatrix} V_R \\ I_R \end{bmatrix} \tag{1.2}$$

Where:

- $A, B, C,$ and D are parameters dependent on the transmission line constants, which will be determined later.
- $A = V_s / V_r$, when $I_r = 0$, i.e., the receiving end is open-circuited. A is therefore a ratio of two voltages (dimensionless).
- $B = V_s / I_r$, when $V_r = 0$, i.e., the receiving end is short-circuited. B has the dimension of impedance (ohm).
- $C = I_s / V_r$, when $I_r = 0$, i.e., the receiving end is open-circuited. C has the dimension of admittance.
- $D = I_s / I_r$, when $V_r = 0$, i.e., the receiving end is short-circuited. D is a ratio of two currents (dimensionless).

The voltage and current at the source end are obtained as follows:

From Figure (1.6):

$$I_L = I_R + Y \cdot V_R \tag{1.3}$$

The source voltage is:

$$V_S = V_R + Z \cdot I_L \tag{1.4}$$

Replacing (1.3) in (1.4), we get:

$$V_S = (1 + ZY)V_R + ZI_R \tag{1.5}$$

The source current is:

$$I_S = I_L + Y \cdot V_S \tag{1.6}$$

By substituting (1.3) and (1.5) into (1.6), we obtain:

$$I_S = Y(1 + ZY/2)V_R + (1 + ZY/2)I_R \tag{1.7}$$

Equations (1.5) and (1.6) can be rewritten in matrix form as:

$$\begin{bmatrix} V_S \\ I_S \end{bmatrix} = \begin{bmatrix} (1 + ZY/2) & Z \\ Y(1 + ZY/2) & (1 + ZY/2) \end{bmatrix} \begin{bmatrix} V_R \\ I_R \end{bmatrix} \tag{1.8}$$

By identifying equations (1.2) and (1.8), we get:

$$A = D = (1 + ZY/2), \quad B = Z, \quad C = Y(1 + ZY/2) \tag{1.9}$$

c) Power transformers:

In electrical networks, power transformers are essential static devices operating at various voltage levels. They modify alternating electrical energy to optimize it for different stages, including power generation, high-voltage (HV) transmission—where they help reduce line losses—and medium-voltage (MV) and low-voltage (LV) distribution. When represented as a non-symmetrical π quadrupole, the transformation ratio is incorporated into the elements of the admittance matrix, making the susceptance values functions of these ratios **[4]**.

.

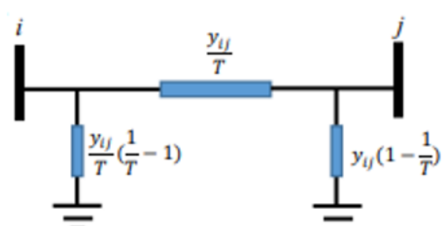

Figure 1.7: *π model of a power transformer*

The admittance matrix of a transformer connected between the node i and node j is given by:

$$Y_t = \begin{bmatrix} y_{ij} & -y_{ij}/a \\ -y_{ij}/a & y_{ij}/a^2 \end{bmatrix} \tag{1.10}$$

d) Electrical load:

The characteristics of electrical loads significantly influence the stability and dynamics of power systems. However, due to their complexity, continuous variation, and the difficulty of obtaining precise data, accurately modeling them is challenging. As a result, simplified models are often necessary, depending on the study's objectives.

In many cases, loads are connected to the electrical network through a load-tap changing transformer, which maintains a nearly constant voltage. For stability studies—where the time frame considered is typically around 10 seconds after a disturbance—the most commonly used models are static **[4]**. These models represent loads using purely algebraic equations, where active and reactive power remain constant and independent of nodal voltage:

$$S_{Di} = P_{Di} + jQ_{Di} \qquad (1.11)$$

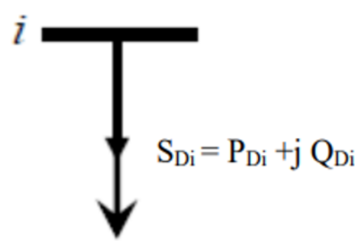

Figure 1.8: *Electrical load model*

Where:

- S_{Di}: Apparent power demanded at bus i.
- P_{Di}: Active power demanded at bus i.
- Q_{Di}: Reactive power; this reactive power can be positive or negative, depending on whether the load is inductive or capacitive.

e) Shunt Elements:

Shunt elements, primarily capacitor banks and reactors, play a crucial role in voltage regulation and reactive power compensation within electrical power systems. These components help maintain system stability by either supplying or absorbing reactive power as needed **[4]**.

- Capacitor Banks: These are used to inject reactive power into the system, effectively increasing voltage levels. They are commonly installed in transmission and distribution networks to improve power factor, reduce losses, and enhance voltage stability.
- Reactors: These function oppositely, absorbing excess reactive power to prevent overvoltage conditions. They are often used in high-voltage networks to control voltage rise, particularly during light-load conditions.

Mathematically, shunt elements are modeled as admittances Y_i, which describe their impact on the system in terms of conductance g_i and susceptance b_i , expressed as:

$$Y_i = g_i + jb_i \qquad (1.12)$$

- g_i (conductance) represents real power losses in the element, often negligible for capacitors and reactors.
- b_i (susceptance) determines the reactive power contribution, with capacitors having positive b_i values (supplying reactive power) and reactors having negative b_i values (absorbing reactive power).

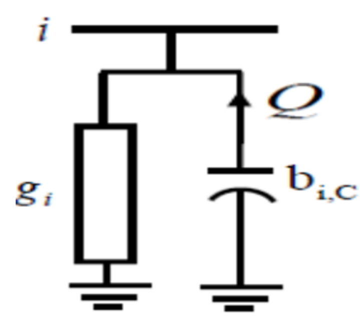

Figure1.9: *Inductive-Capacitive Shunt Element Model*

1.7 Electrical Network Node Classification and Modeling:

In power system analysis, electrical network nodes are classified into different types based on their role in the system. This classification is essential for solving power flow equations and ensuring proper system operation. The three main types of nodes are:

a) P-V Generator Node (Voltage-Controlled Node):

This type of node is associated with power generation plants, where the active power and voltage magnitude are specified. These nodes help regulate the system voltage within acceptable limits. The unknown variables to be determined at these nodes are the voltage phase angle and the reactive power. Voltage-controlled nodes are crucial for maintaining system stability and ensuring an efficient power distribution.

b) P-Q Load Node (Load Node):

These nodes are generally associated with electrical loads, representing points where power is consumed. The active power and reactive power are known parameters, as they are dictated by the demand at that particular node. However, the voltage magnitude and phase angle must be determined through power flow calculations. In some cases, generators with fixed active and reactive power outputs may also be connected to P-Q nodes. These nodes are the most common in a power system, as they model the various consumer loads.

c) Slack Bus (Reference Node or V-θ Node):

The slack bus serves as a reference point for voltage and phase angle in the system. It is typically associated with the most powerful generation plant, which compensates for any mismatches in generation and demand within the network. At the slack bus, the voltage magnitude and phase angle are specified, while the active power and reactive power are the unknowns that need to be determined. The slack bus plays a crucial role in ensuring power balance and maintaining system stability, as it absorbs any deviations in power flow caused by losses or variations in generation and load.

1.8 Protection of Electrical Networks:

The protection of an electrical network is essential to ensure the reliability, stability, and safety of power systems. Protection devices continuously monitor the electrical state of network components and disconnect them from the power supply when an undesirable disturbance occurs. Such disturbances can include short circuits, insulation failures, overvoltage, frequency deviations, overloads, and ground faults **[5]**. The primary goal of network protection is to minimize damage to equipment, prevent cascading failures, and maintain service continuity.

a) Principle of Network Protection:

When a fault occurs in an electrical network, multiple protection devices located in different areas of the system may detect the anomaly simultaneously. Their selective tripping mechanism ensures that only the faulty section is isolated as quickly as possible, while the rest of the network remains operational. This selectivity is crucial for reducing downtime, preventing unnecessary power outages, and limiting the risk of widespread blackouts **[5]**.

b) Types of Protection Devices:

Protection functions are carried out by specialized devices such as protection relays, circuit breakers, fuses, and multifunctional protection systems.

- **Protection Relays**: Initially, these devices were analog and typically performed a single function, such as overcurrent or differential protection.
- **Digital (Numerical) Relays**: With advancements in digital technology, modern protection systems incorporate programmable digital relays that can execute multiple protection functions within a single device. These multifunctional relays enhance the efficiency and flexibility of network protection.
- **Circuit Breakers**: These are key components of network protection, automatically interrupting the current flow when a fault is detected.
- **Fuses**: Primarily used in low-voltage networks, fuses provide overcurrent protection by melting and breaking the circuit when excessive current flows through them.
- **Differential Protection**: This technique is widely used in transformers, generators, and transmission lines, ensuring that only faulty components are disconnected.

c) Advanced Protection Strategies:

Modern power systems employ advanced protection strategies, such as:

- **Adaptive Protection Systems**: These systems dynamically adjust protection settings based on real-time network conditions.
- **Distance Protection**: Used in transmission lines, this method detects faults based on the impedance between the fault location and the relay.
- **Overcurrent and Earth Fault Protection**: Essential for detecting abnormal currents caused by faults or leakage currents.

d) Characteristics of an Effective Protection System:

To ensure high performance, a protection system must meet the following key criteria:

- **Speed** – The ability to detect and isolate faults quickly, minimizing damage and preventing further complications.
- **Selectivity** – Ensuring that only the faulty section is disconnected, preserving the rest of the network and reducing unnecessary disruptions.
- **Sensitivity** – The capability to detect even minor faults while avoiding false tripping.
- **Reliability** – Ensuring both the safety of personnel and the stability of the electrical network under all operating conditions.

With the increasing integration of renewable energy sources and smart grids, modern protection systems must continuously evolve to accommodate new challenges, including bidirectional power flows, distributed generation, and cybersecurity threats. The implementation of artificial intelligence (AI) and machine learning (ML) in protection relays is expected to further improve fault detection accuracy and reduce response time, making future networks even more resilient and efficient **[6]**.

1.9 Conclusion:

In this chapter, we discussed the different types of electrical networks and detailed their structures through various topologies, highlighting their advantages and disadvantages.

We then examined the classification of voltage levels and the modeling of key components such as generators, transmission lines, transformers, and electrical loads.

We also introduced the per-unit system, which simplifies power system calculations by expressing electrical quantities relative to chosen base values.

Finally, we covered an essential aspect of electrical networks: their protection, including key protection devices and systems used to ensure network stability and reliability.

Chapter 2:

Modeling of Radial Electrical Networks

2.1 Introduction:

Modeling a radial distribution network is an important step in performing accurate power flow analysis and assessing the electrical behavior of the system. The 34-bus test network used in this study reflects a typical radial structure commonly found in medium-voltage distribution systems. Its configuration, based on a single source feeding multiple downstream load buses, allows for the application of efficient power flow methods tailored to radial topologies. To analyze the electrical parameters and system performance, two techniques are used, the Backward-Forward Sweep method, known for its suitability to radial networks, and the Loss Sensitivity Index (LSI), which assists in identifying critical buses and evaluating voltage sensitivity across the system. Modeling assumptions and the simulation framework are also discussed **[7]**.

2.2 Description of the 34-Bus Test System:

The system of our study consists of a radial distribution network comprising 34 buses and multiple lateral branches, forming a tree-like structure fed from a single source at Bus 1. The topology reflects typical medium-voltage distribution systems, with power flowing unidirectionally from the source through the main feeder and branching laterally to reach downstream buses. Several branches emerge from buses such as 3, 6, 7, and 10, extending the network both vertically and horizontally, as shown in (Figure 2.1). The network includes both short and long feeders, as well as zones with relatively dense bus clusters, which present various load distribution and voltage profile challenges.

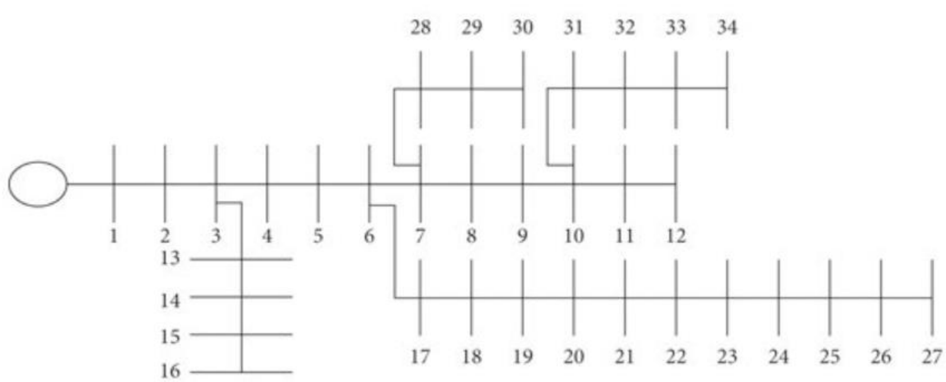

Figure 2.1: *IEEE 34-Bus Radial Distribution Test System*

2.3 Power Flow Problem Formulation:

The power flow problem, also known as load flow analysis, aims to determine the steady-state operating conditions of an electrical power system under a given load configuration. Specifically, it involves calculating the voltage magnitude V_i and phase angle δ_i at each bus, as well as the power flows through each line, given known load and generation values **[8, 9]**.

Each bus in the system is associated with four variables: active power P_i, reactive power Q_i, voltage magnitude V_i, and voltage phase angle δ_i. Depending on the bus type (PQ, PV, or slack), two of these variables are known, and the other two must be computed. The solution of the power flow problem consists of finding a consistent set of voltages and angles that satisfy the power balance equations at every bus **[8, 9]**.

For each bus i, the nonlinear power balance equations are:

$$P_i = V_i \sum_{j=1}^{n} V_j \left(G_{ij}\cos(\delta_i - \delta_j) + B_{ij}\sin(\delta_i - \delta_j)\right) \quad (2.1)$$

$$Q_i = V_i \sum_{j=1}^{n} V_j \left(G_{ij}\sin(\delta_i - \delta_j) - B_{ij}\cos(\delta_i - \delta_j)\right) \quad (2.2)$$

Where:

- P_i, Q_i: Net active and reactive power injected at bus i
- V_i, V_j: Voltage magnitudes at buses i and j
- δ_i, δ_j: Voltage phase angles at buses i and j
- G_{ij}, B_{ij}: Real and imaginary parts of the admittance matrix Y_{ij}
- n: Total number of buses in the system

These equations are nonlinear due to the trigonometric terms and the products of voltage magnitudes, making analytical solutions impractical for large systems. Iterative numerical methods are therefore employed to solve the equations **[8]**.

In radial distribution systems, several characteristics differentiate the power flow problem from that of transmission systems:

- The R/X ratio is typically high, making conventional methods like Newton-Raphson less effective.
- The topology is tree-like and unbalanced in practice (though usually modeled as balanced in single-phase analysis).
- Voltage drops and power losses are more pronounced.

To account for these challenges, specialized algorithms such as the Backward-Forward Sweep method and sensitivity-based techniques (e.g., Loss Sensitivity Index) are commonly used.

2.4 Applied Power Flow Techniques:

a) Sensitivity Analysis and Loss Sensitivity Indices (LSIs):

Two Loss Sensitivity Indices (LSIs) are used to rank load buses based on their severity, aiding in the efficient identification of candidate buses for capacitor installation. The purpose of selecting these candidate buses is to minimize the search space in the optimization process **[10]**.

In a radial distribution system, we consider two nodes connected by a branch, as shown in Figure 3.2, where bus p is the sending end and bus q is the receiving end **[10]**.

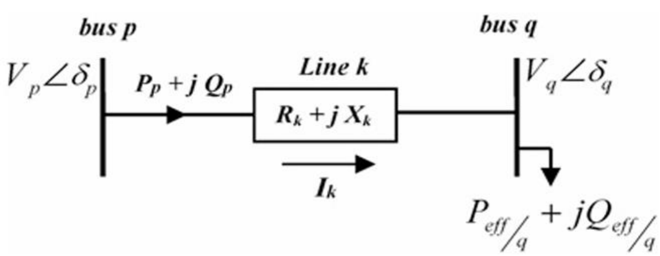

Figure 2.2: *Representation of two nodes*

The active power P_n and reactive power Q_n flowing through a branch k from node p to node q can l

$$P_p = P_{\mathrm{eff/q}} + P_{\mathrm{Loss},k} \quad (2.3)$$

$$Q_p = Q_{\mathrm{eff/q}} + Q_{\mathrm{Loss},k} \quad (2.4)$$

Where:

- P_p and Q_p are the power flows through branch k.
- $P_{\mathrm{eff/q}}$ and $Q_{\mathrm{eff/q}}$ are the total effective active and reactive power loads beyond node q, respectively.
- $P_{\mathrm{Loss},k}$ and $Q_{\mathrm{Loss},k}$ are the active and reactive power losses through branch k, respectively.

The current flowing through branch k from node p to node q can be calculated as:

$$I_k = \frac{P_p - jQ_p}{V_p\angle - \delta_p} \qquad (2.5)$$

Also,

$$I_k = \frac{V_p\angle\delta_p - V_q\angle\delta_q}{R_k + jX_k} \qquad (2.6)$$

Let V_p and V_q be the voltage magnitudes at nodes p and q, respectively, and let δ_p and δ_q be the voltage angles at these nodes. The parameters R_k and X_k represent the resistance and reactance of branch k, respectively.

From equations (11) and (12), we derive the following equation:

$$V_p^2 - V_pV_q(\delta_q - \delta_p) = \frac{P_p - jQ_p}{R_k + jX_k} \qquad (2.7)$$

By equating the real and imaginary parts, we obtain:

$$V_pV_q\cos(\delta_q - \delta_p) = V_p^2 - (P_pR_k + Q_pX_k) \qquad (2.8)$$

$$V_pV_q\sin(\delta_q - \delta_p) = Q_pR_k - P_pX_k \qquad (2.9)$$

Squaring and adding these equations results in:

$$V_q^2 = V_p^2 - 2\frac{P_pR_k + Q_pX_k + R_k^2 + X_k^2}{V_p^2}(P_p^2 + Q_p^2) \qquad (2.10)$$

The active and reactive power losses in branch k are calculated as:

$$P_{\text{Loss},k} = I_k^2R_k = \left(\frac{P_{\text{eff}/q}^2 + Q_{\text{eff}/q}^2}{V_q^2}\right)R_k \qquad (2.11)$$

$$Q_{\text{Loss},k} = I_k^2X_k = \left(\frac{P_{\text{eff}/q}^2 + Q_{\text{eff}/q}^2}{V_q^2}\right)X_k \qquad (2.12)$$

For the entire radial distribution system, the total active and reactive power losses are:

$$\text{Total } P_{\text{Loss}} = \sum_{q=2}^{N_b}\sum_{k=1}^{N_b-1}\frac{P_{\text{eff}/q}^2 + Q_{\text{eff}/q}^2}{V_q^2}R_k \qquad (2.13)$$

$$\text{Total } Q_{\text{Loss}} = \sum_{q=2}^{N_b}\sum_{k=1}^{N_b-1}\frac{P_{\text{eff}/q}^2 + Q_{\text{eff}/q}^2}{V_q^2}X_k \qquad (2.14)$$

where $P_{\text{eff}/q}$ and $Q_{\text{eff}/q}$ are the total effective active and reactive power loads beyond node q, respectively. N_b is the total number of system buses, and $N_b - 1$ represents the total number of branches.

- **First Loss Sensitivity Index (LSI1):**

By differentiating $P_{\text{Loss},k}$ (2.11) with respect to V_q while considering $P_{\text{eff}/q}$, $Q_{\text{eff}/q}$, and R_k as constants, we obtain:

$$\text{LSI1} = \frac{\partial P_{\text{Loss},k}}{\partial V_q} = -2R_k \frac{P_{\text{eff}/q}^2 + Q_{\text{eff}/q}^2}{V_q^3} \qquad (2.15)$$

The values of LSI1 represent the highest and lowest performance indices. Buses with the largest negative LSI1 values are identified as the most suitable candidates for capacitor installation and are ranked at the top of the LSI1 list. In contrast, buses with the smallest negative LSI1 values are placed at the bottom of the list, as they exhibit lower sensitivity for capacitor placement **[10, 11]**.

- **Second Loss Sensitivity Index (LSI2):**

The second loss sensitivity index (LSI2) is obtained by differentiating $P_{\text{Loss},k}$ (2.11) with respect to $Q_{\text{eff}/q}$.

we obtain:

$$\text{LSI2} = \frac{\partial P_{\text{Loss},k}}{\partial Q_{\text{eff}/q}} = 2\frac{Q_{\text{eff}/q} R_k}{V_q^2} \qquad (2.16)$$

Similarly, buses with the largest positive values of LSI2 are considered candidate buses for capacitor installation. These buses are indexed at the top of the LSI2 list, while buses with the smallest positive values of LSI2 are placed at the bottom, indicating lower sensitivity for capacitor placement.

b) Backward/Forward Sweep (BFS) Algorithm:

The BFS algorithm is one of the most common methods used for load flow analysis in a distribution system due to its simplicity, fast and robust convergence, and low memory requirements while maintaining computational efficiency and solution accuracy **[10, 12]**.

The BFS algorithm involves three iterative steps based on Kirchhoff's Current Law (KCL) and Kirchhoff's Voltage Law (KVL) **[12]**:

- Nodal current calculation
- Backward sweep
- Forward sweep

These steps are repeated until convergence is achieved. The BFS method also utilizes a simple and flexible radial distribution system numbering scheme to assign numbers to each branch in the feeder, lateral, and sub-lateral **[13]**.

The BFS algorithm follows these steps to find the load flow results:

Step 1: Initialization

The following data is inserted:

- Distribution system line and load data
- Base power and base voltage
- Calculation of base impedance
- Per-unit values of line and load data
- Flat voltage initialization for all buses (1.0 P.U.)
- Convergence tolerance $\varepsilon = 0.0001$ and $\Delta V_{\max} = 0$.

Step 02: Nodal Current Injection and Voltage Calculation

The nodal current and voltage are computed using the following equations:

$$I_{\text{Line}}^{i} = \frac{P_p - jQ_p}{V_p^*} \quad (2.17)$$

$$V_q^i = V_p^i - Z_{\text{Line}}^i \times I_{\text{Line}}^i \quad (2.18)$$

Step 03: Evaluation

The assessment is based on the following criteria:

- **Voltage Difference:**

$$\Delta V_i^{\text{iter}} = |V_i^{\text{iter}}| - |V_i^{\text{iter}-1}| \quad (2.19)$$

- **Power Loss Calculation:**

Using Equations (2.13) and (2.14).

- **Loss Sensitivity Indices:**

Derived from Equations (2.15) and (2.16).

Step 04: Criterion

Set a convergence tolerance $\Delta V_{\max} \leq \varepsilon$.

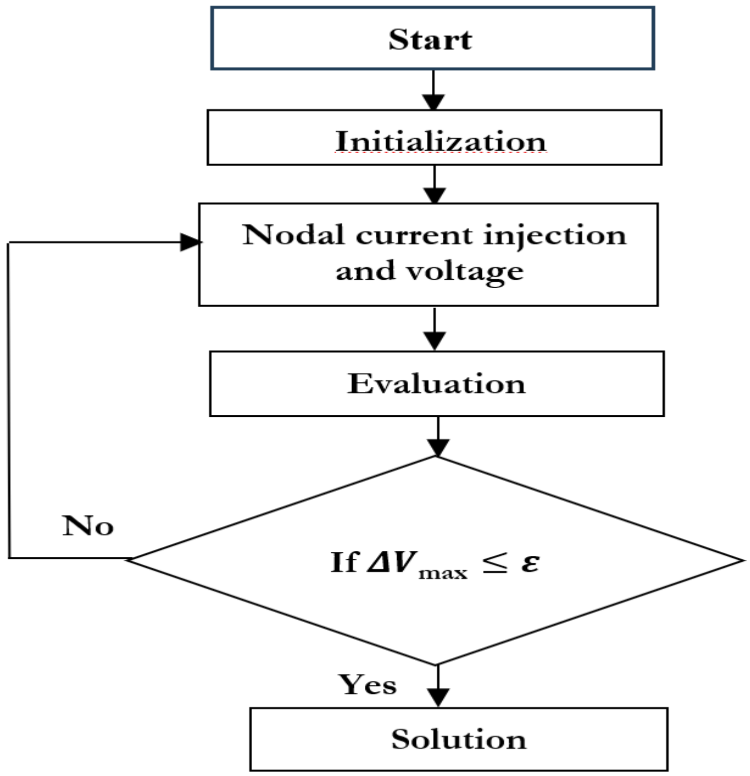

Figure 2.3: *Flow chart of BFS load flow*

2.5 Conclusion:

In this chapter, a 34-bus radial distribution network was modeled and analyzed to reflect the characteristics of typical medium-voltage systems. All buses, except for the slack bus, were modeled as PQ buses with constant power loads to simplify and standardize the analysis. Due to the radial topology and high R/X ratio, conventional methods were less suitable; therefore, the Backward-Forward Sweep (BFS) method and Loss Sensitivity Indices (LSIs) were employed.

The BFS algorithm provided an efficient and robust approach for load flow calculations, while the LSI methods helped identify candidate buses for reactive power compensation, particularly for capacitor placement. Together, these techniques enhance the accuracy of power flow analysis and support future optimization efforts aimed at reducing losses and improving voltage profiles across the network.

Chapter 3: Metaheuristic Methods

3.1 Introduction:

In recent decades, the increasing complexity of electrical distribution networks—driven by the integration of renewable energy sources, distributed generation, and smart grid technologies—has posed significant challenges for traditional optimization methods. These networks must now operate more efficiently, reliably, and flexibly, all while meeting environmental and economic constraints.

Classical optimization techniques often struggle to handle the nonlinear, large-scale, and multi-constrained nature of these modern systems. To address this, the research community has turned to more adaptable and intelligent solution strategies.

Among these, metaheuristic algorithms have emerged as powerful tools capable of exploring complex solution spaces efficiently. Widely used across engineering and computational disciplines, these algorithms have proven particularly effective for solving problems in power systems, such as optimal power flow, network reconfiguration, and power loss minimization.

3.2 Definition and Classifications of Metaheuristic Algorithms:

a) Definition of Metaheuristic Algorithms:

Metaheuristic methods are algorithmic frameworks designed to find optimal solutions to complex optimization problems. These methods provide approximate solutions within a reasonable computational time. This makes them very valuable in real-world applications where time, flexibility, and adaptability are critical **[14]**.

The term *metaheuristic* itself is derived from the Greek words *meta* (meaning "beyond" or "higher level") and *heuristic* (meaning "to discover"), highlighting their role as generalized strategies that guide the search process across different problem domains. These methods do not require strict mathematical formulations, which allows them to be applied to a wide variety of discrete, continuous, and mixed-variable problems **[14]**.

Metaheuristics are especially powerful in solving nonlinear optimization problems where traditional methods struggle, including highly constrained or multi-objective problems

[14, 15]. They are frequently inspired by processes found in nature or human behavior, such as evolution, swarm behavior, thermodynamics, or predator-prey interactions, and operate through mechanisms like exploration (global search) and exploitation (local refinement) **[15]**.

Though there is a wide range of metaheuristic techniques (which will be detailed in the next section), they generally fall into two broad philosophies: single-solution-based (trajectory methods) and population-based methods. However, this categorization serves more as a conceptual guide, as many modern approaches blend features from multiple families.

Metaheuristic methods offer several advantages that make them attractive for solving complex optimization problems. They are problem-independent, meaning they can be applied across a wide range of domains without requiring extensive customization. Their flexibility allows them to handle diverse constraints and objective functions with ease. Many metaheuristics are also scalable, making them suitable for large-scale or high-dimensional problems. Additionally, they are typically easy to implement and fine-tune **[15]**. Perhaps most importantly, their global search capability enables them to escape local optima, increasing the likelihood of finding high-quality solutions.

Despite these advantages, metaheuristics do not guarantee an optimal solution, and their performance can depend on algorithm-specific parameters and problem context. Nevertheless, their balance between solution quality and computational efficiency has made them a vital tool in modern optimization, particularly in fields such as engineering design, energy systems, logistics, machine learning, and network optimization.

b) Classification of Metaheuristic Methods:

Metaheuristic optimization methods can be classified in various ways depending on their search strategies, sources of inspiration, and structural characteristics. One of the most practical and widely accepted classifications groups these methods into three main categories: trajectory-based methods, swarm intelligence algorithms, and evolutionary-based algorithms. This classification reflects key differences in how these approaches explore the solution space, manage populations, and draw inspiration from natural or artificial systems.

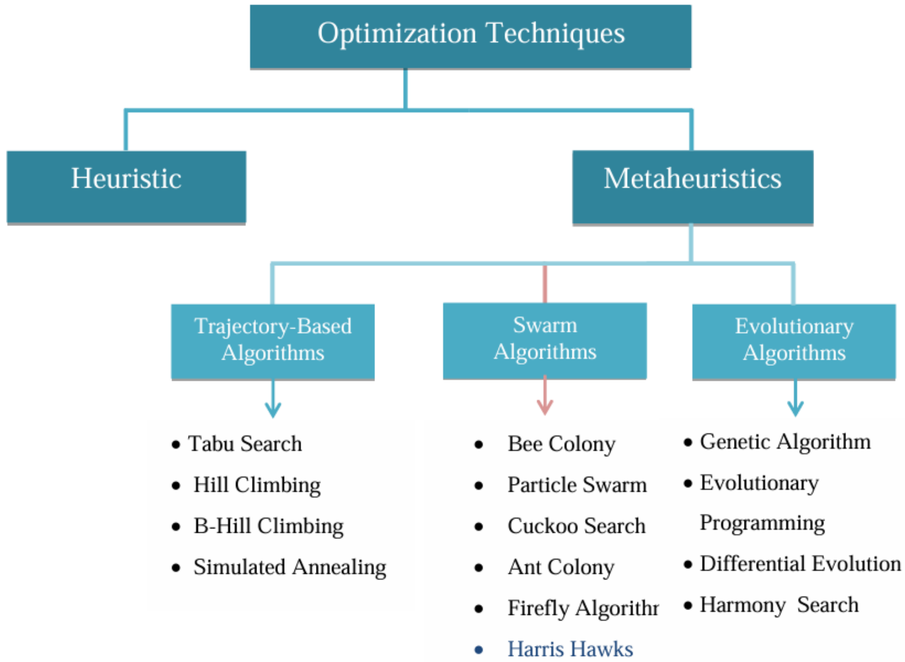

Figure 3.1*Classification of metaheuristic methods*

c) Trajectory-Based Metaheuristic Methods:

Trajectory-based metaheuristic methods focus on the iterative improvement of a single solution over time. These algorithms explore the solution space by generating a sequence of solutions, referred to as a trajectory—through local or global modifications. At each step, the current solution is updated based on predefined rules guided by randomness and memory mechanisms to help escape local optima **[15, 16]**.

Unlike population-based methods, trajectory-based approaches do not maintain multiple candidate solutions simultaneously. Instead, they focus computational effort on refining one solution path, which can be advantageous in terms of simplicity and memory efficiency.

Examples of trajectory-based metaheuristics include:

i) Simulated Annealing (SA):

Inspired by the annealing process in metallurgy, SA probabilistically accepts worse solutions during the search to escape local minima, gradually reducing this behavior as the algorithm progresses **[16]**.

ii) Tabu Search:

Uses a memory structure (tabu list) to avoid revisiting previously explored solutions, encouraging the search to move into unexplored areas of the solution space **[16]**.

iii) Iterated Local Search (ILS):

Applies a local search repeatedly from perturbed versions of the current solution to avoid getting stuck in suboptimal regions **[16]**.

These methods are particularly useful for problems where maintaining a population is unnecessary or too costly, and where a well-guided single-solution search can yield competitive results.

d) Swarm Intelligence Algorithms:

Swarm intelligence algorithms are a subset of metaheuristic methods inspired by the collective behavior of systems in nature—such as bird flocking, fish schooling, or ant colonies. These algorithms rely on the interaction of multiple simple particles that cooperate to explore the solution space without any central control **[15, 17]**.

Each particle follows simple rules and communicates with others (directly or indirectly), enabling the swarm to collectively converge toward better solutions over time **[19, 20]**. The strength of swarm algorithms lies in their ability to balance exploration and exploitation, making them suitable for complex optimization problems, below are some Common Swarm Intelligence Algorithms:

i) Particle Swarm Optimization (PSO):

- Inspired by bird flocking or fish schooling.
- Each particle represents a solution and moves through the solution space influenced by its own experience and that of its neighbors **[17]**.

ii) Ant Colony Optimization (ACO):

- Mimics the behavior of ants, using artificial pheromones to guide solution construction.
- Well-suited for combinatorial problems like the Traveling Salesman Problem **[17]**.

iii) Artificial Bee Colony (ABC):

- Based on the food foraging behavior of honey bees.
- Divides agents into employed, onlooker, and scout bees to explore and exploit food sources (i.e., solutions) **[17]**.

iv) Harris Hawks Optimization (HHO):

- A newer swarm-based algorithm inspired by the cooperative hunting strategy of Harris' hawks.
- It simulates dynamic attack behaviors and is effective at balancing diversification and intensification during the search process **[18]**.

Swarm algorithms are population-based and often excel in problems where a balance between global search and local refinement is essential. Their decentralized nature also makes them robust and adaptable to changing environments.

Both Particle Swarm Optimization (PSO) and Harris Hawks Optimization (HHO) fall under this category of swarm intelligence methods. These two algorithms will be discussed in more detail in the following sections, as they play a central role in our work.

e) Evolutionary-Based Algorithms:

Evolutionary-based algorithms are inspired by the process of natural evolution and survival of the fittest. The algorithms operate on a population of candidate solutions and apply mechanisms such as selection, crossover (recombination), and mutation to evolve better solutions over successive generations **[14, 15]**.

The core idea is to simulate the biological evolutionary process to explore and exploit the search space. Solutions that perform better are given a higher chance to contribute to the next generation, allowing the population to gradually converge toward optimal or near-optimal solutions.

i) Genetic Algorithms (GA):

- Mimic biological evolution using selection, crossover, and mutation.
- Widely used for both combinatorial and continuous optimization problems **[18]**.

ii) Evolution Strategies (ES):

Emphasize self-adaptation and mutation as key drivers of search, often used for real-valued parameter optimization.

iii) Differential Evolution (DE):

Uses vector differences for mutation and relies on a simple yet powerful scheme for global optimization **[19]**.

Evolutionary algorithms can be adapted to a variety of problem types, including discrete, continuous, and multi-objective optimization. Their ability to maintain diversity in the population helps them avoid premature convergence and escape local optima **[14]**.

These algorithms, while distinct from swarm intelligence approaches, share the population-based structure and are often compared or even hybridized with swarm-based methods for better performance.

3.3 Particle Swarm Optimization:

Particle swarm optimization (PSO) is one of the bio-inspired algorithms and it is a simple one to search for an optimal solution in the solution space. It is different from other optimization algorithms in such a way that only the objective function is needed and it is not dependent on the gradient or any differential form of the objective **[19]**. It also has very few hyperparameters.

Particle Swarm Optimization was proposed by Kennedy and Eberhart in 1995. As mentioned in the original paper, sociobiologists believe a school of fish or a flock of birds that moves in a group “can profit from the experience of all other members”. In other words, while a bird flying and searching randomly for food, for instance, all birds in the flock can share their discovery and help the entire flock get the best hunt **[19]**.

While we can simulate the movement of a flock of birds, we can also imagine each bird is to help us find the optimal solution in a high-dimensional solution space and the best solution found by the flock is the best solution in the space **[19]**. This is a heuristic solution because we can never prove the real global optimal solution can be found and it is usually not. However, we often find that the solution found by PSO is quite close to the global optimal.

a) Phases of Particle Swarm Optimization (PSO)

While Particle Swarm Optimization (PSO) is not originally divided into distinct operational phases, its behavior throughout the optimization process naturally aligns with three intuitive stages: Exploration, Transition, and Exploitation. These phases reflect the gradual shift in particle behavior from broadly scanning the search space to fine-tuning around the best-found solutions. Each stage plays a critical role in achieving a balance between global search and local refinement **[20]**.

i) Exploration Phase

In the initial stage of PSO, the algorithm focuses on exploration—encouraging particles to investigate diverse areas of the search space. This is primarily achieved by assigning a high inertia weight (ω), which allows particles to maintain momentum from their previous movements. The goal is to avoid premature convergence by preventing particles from quickly clustering around suboptimal solutions **[17]**.

The velocity and position of each particle are updated using the standard PSO equations:

$$v_i^{(t+1)} = \omega v_i^{(t)} + c_1 r_1 \left(pbest_i - x_i^{(t)}\right) + c_2 r_2 \left(gbest - x_i^{(t)}\right) \quad (3.1)$$

$$x_i^{(t+1)} = x_i^{(t)} + v_i^{(t+1)} \quad (3.2)$$

Here, $v_i^{(t)}$ and $x_i^{(t)}$ denote the velocity and position of particle i at iteration t, respectively; $pbest_i$ represents the best-known position of particle i, and $gbest$ is the best-known position among all particles. The constants c_1 and c_2 are the cognitive and social acceleration coefficients, while r_1 and r_2 are uniformly distributed random numbers in [0, 1]. During this phase, the influence of $pbest$ and $gbest$ is relatively small compared to the inertia component, allowing broad exploration of the search space **[17,21]**.

ii) Transition Phase

As the optimization process progresses, PSO enters a transition phase in which it gradually shifts from exploration to exploitation. This is typically managed by dynamically decreasing the inertia weight over iterations. A common approach is to apply a linear inertia weight decay **[17]**:

$$\omega = \omega_{max} - \left(\frac{\omega_{max} - \omega_{min}}{t_{max}}\right) \cdot t \qquad (3.3)$$

where ω_{max} and ω_{min} are the maximum and minimum inertia values, t is the current iteration number, and t_{max} is the total number of iterations. Reducing the inertia weight gradually decreases the particles' tendency to explore and increases their responsiveness to personal and global best positions. This balancing act ensures that the swarm begins to focus its efforts on promising areas of the solution space without becoming trapped too early.

iii) Exploitation Phase

In the final stage, the algorithm concentrates on exploitation, refining the search around the most promising solutions found thus far. With a low inertia weight, the influence of the social ($gbest$) and cognitive ($pbest$) components becomes dominant. This causes particles to converge toward the best-known areas, effectively performing a local search to fine-tune the solution **[20, 21]**.

Although the velocity and position equations remain unchanged, the behavior of the swarm becomes increasingly exploitative due to parameter adjustments and decreased velocity. This phase aims to improve precision and convergence accuracy, ultimately leading to the discovery of optimal or near-optimal solutions.

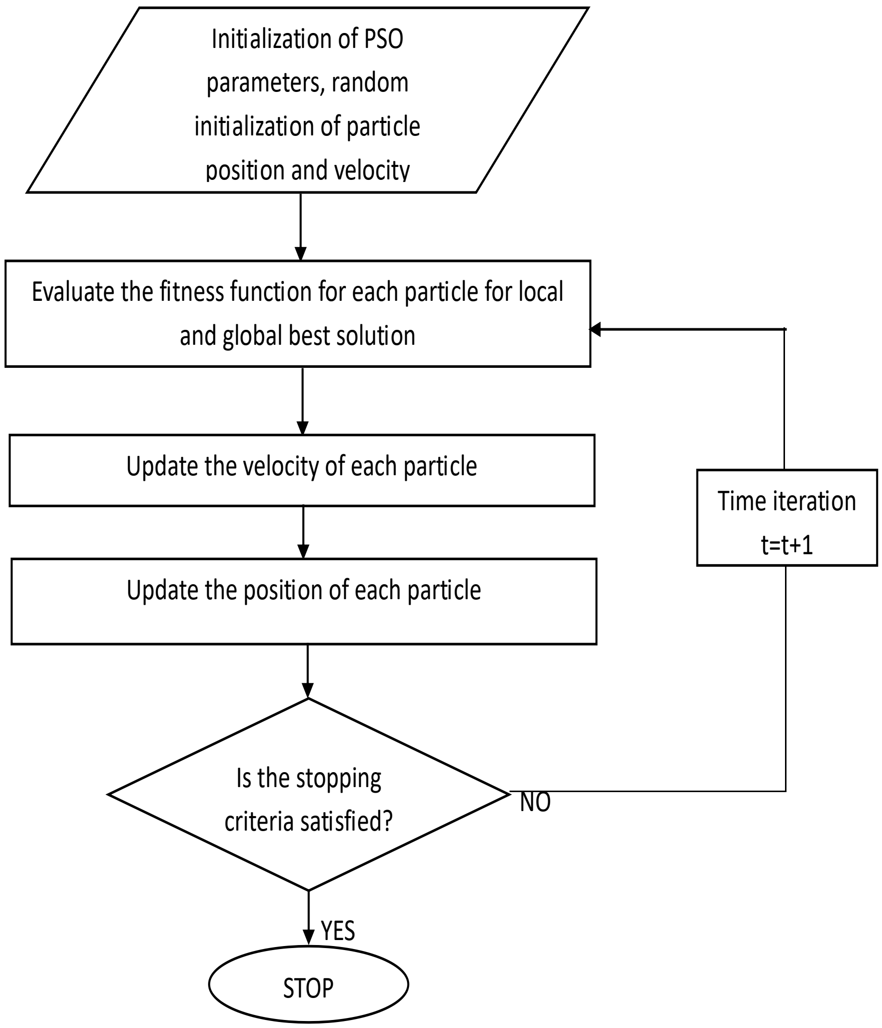

Figure 3.2: *Flow chart of Particle Swarm Optimization Algorithm (PSO)*

3.4 Harris Hawks Optimization (HHO):

Harris Hawks Optimization is a popular swarm-based, gradient-free optimization algorithm with several active and time-varying phases of exploration and exploitation. This algorithm initially published by the Journal of Future Generation Computer Systems (FGCS) in 2019, and from the first day, it has gained increasing attention among researchers due to its flexible structure, high performance, and high-quality results. The main logic of the HHO method is designed based on the cooperative behavior and chasing styles of Harris' hawks in nature called "surprise pounce". Currently, there are many suggestions about how to enhance the functionality of HHO, and there are also several enhanced variants of the HHO in the leading Elsevier and IEEE transaction journals **[22]**.

From the algorithmic behavior viewpoint, there are several effective features in HHO: Escaping energy parameter has a dynamic randomized time-varying nature, which can further improve and harmonize the exploratory and exploitive patterns of HHO **[18]**. This factor also supports HHO to conduct a smooth transition between exploration and exploitation. Different exploration mechanisms with respect to the average location of hawks can increase the exploratory trends of HHO throughout initial iterations **[18]**. Diverse LF-based patterns with short-length jumps enrich the exploitative behaviors of HHO when directing a local search. The progressive selection scheme supports search agents to progressively advance their position and only select a better position, which can improve the superiority of solutions and intensification powers of HHO throughout the optimization procedure. HHO shows a series of searching strategies and then, it selects the best movement step. This feature has also a constructive influence on the exploitation inclinations of HHO. The randomized jump strength can assist candidate solutions in harmonizing the exploration and exploitation leanings. The application of adaptive and time-varying components allows HHO to handle difficulties of a feature space including local optimal solutions, multi-modality, and deceptive optima **[18]**.

a) Phases of Harris Hawks Optimization (HHO):

i) Exploration Phase

In the HHO algorithm, Harris hawks randomly perch in various locations while searching for prey. They employ two strategies to do this **[18]**:

If $q \geq 0.5$, the hawks update their positions using:

$$X(t+1) = X_{rand}(t) - r_1|X_{rand}(t) - 2r_2X(t)| \tag{3.4}$$

If $q < 0.5$, the position is updated by:

$$X(t+1) = (X_{rabbit}(t) - X_m(t)) - r_3(LB + r_4(UB - LB)) \tag{3.5}$$

Here:

- $X(t+1)$: position of the hawk in the next iteration
- $X(t)$: current position
- $X_{rabbit}(t)$: position of the prey
- $X_{rand}(t)$: randomly chosen hawk's position
- $X_m(t)$: average position of all hawks
- LB, UB: lower and upper bounds of the search space
- r_1 to r_4 and q: random numbers in the interval (0, 1)

The average hawk position is calculated by:

$$X_m(t) = \frac{1}{N}\sum_{i=1}^{N} X_i\,(t) \qquad (3.6)$$

Where N is the total number of hawks, and $X_i(t)$ is the position of the i-th hawk at iteration t.

ii) Transition from Exploration to Exploitation:

The algorithm mimics the energy level of the prey to determine the transition between exploration and exploitation. The energy is modeled as **[18]**:

$$E = 2E_0\left(1 - \frac{t}{T}\right) \qquad (3.7)$$

Where:

- E: current escaping energy of the prey
- E_0: initial energy
- t: current iteration
- T: maximum number of iterations

iii) Exploitation Phase

➢ **Soft Besiege:**

When the hawks decide to softly encircle the prey, the position is updated as follows:

$$X(t+1) = \Delta X(t) - E|JX_{rabbit}(t) - X(t)| \quad (3.8)$$

Where:

- $\Delta X(t) = X_{rabbit}(t) - X(t)$
- $J = 2(1 - r_5)$ is a random jump strength determined using $r_5 \in (0,1)$

➢ **Hard Besiege:**

When the prey is exhausted and cannot escape effectively, the hawks apply a hard besiege **[18]**:

$$X(t+1) = X_{rabbit}(t) - E|\Delta X(t)| \quad (3.9)$$

➢ **Soft Besiege with Progressive Rapid Dives:**

In this scenario, hawks decide their next position as:

$$Y = X_{rabbit}(t) - E|JX_{rabbit}(t) - X(t)| \quad (3.10)$$

They then perform a dive based on Lévy flight:

$$Z = Y + S \times LF(D) \quad (3.11)$$

Where:

- S: random vector of size $1 \times D$
- $LF(D)$: Lévy flight function, defined as:

$$LF(x) = 0.01 \times \frac{u \cdot \sigma}{|v|^{1/\beta}} \quad (3.12)$$

with $u, v \in (0,1)$, $\beta = 1.5$, and

$$\sigma = \left(\frac{\Gamma(1+\beta)\cdot\sin(\pi\beta/2)}{\Gamma((1+\beta)/2)\cdot\beta\cdot 2^{(\beta-1)/2}}\right)^{1/\beta} \tag{3.13}$$

The hawks then choose the better solution:

$$X(t+1) = \begin{cases} Y & \text{if } F(Y) < F(X(t)) \\ Z & \text{if } F(Z) < F(X(t)) \end{cases} \tag{3.14}$$

- **Hard Besiege with Progressive Rapid Dives:**

In this variant, the hawks encircle the prey based on the average position:

$$Y = X_{rabbit}(t) - E|JX_{rabbit}(t) - X_m(t)| \tag{3.15}$$

$$Z = Y + S \times LF(D) \tag{3.16}$$

The new position is selected using the same rule as in the soft besiege with dives.

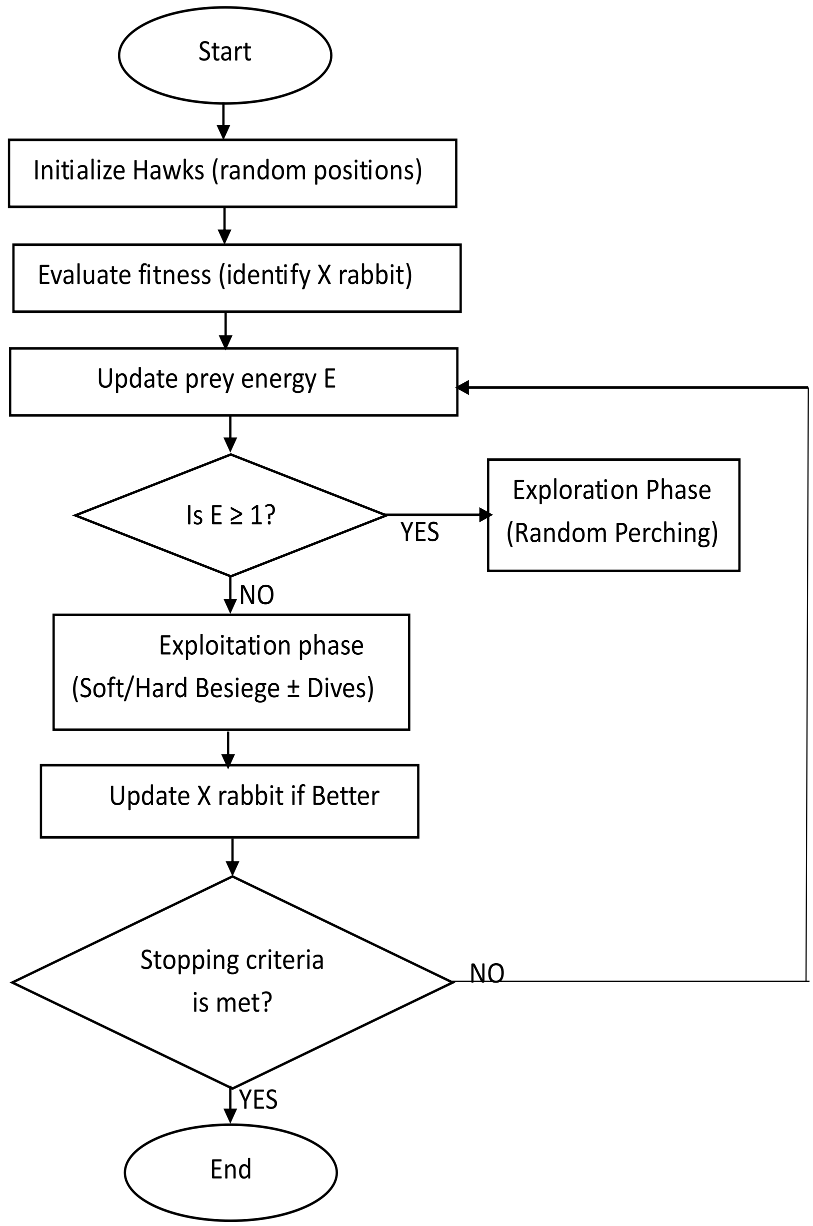

Figure 3.3: *Flow Chart of Harris Hawks Optimization Algorithm (HHO)*

3.5 Conclusion:

In this chapter, we provided a general introduction of metaheuristic optimization methods, and their main classifications, focusing on three prominent categories: trajectory-based methods, swarm intelligence algorithms, and evolutionary-based approaches. Within the swarm-based category, there are the two optimization techniques used in this study—Particle Swarm Optimization (PSO) and Harris Hawks Optimization (HHO)—laying the groundwork for the detailed analysis and application of each in the upcoming sections.

Chapter 4: Results and Discussions

4.1 Introduction:

This chapter presents the numerical and graphical results, discussions, and interpretations of our two-stage approach for determining the optimal placement and sizing of capacitors in a radial distribution system. In the first stage, loss sensitivity analysis is conducted using two loss sensitivity indices (LSIs) to identify the most suitable locations for capacitor installation. In the second stage, Harris Hawks and the particle swarm optimization algorithm are employed to determine the optimal capacitor placement and sizing while minimizing energy losses and capacitor costs, ensuring all system constraints are met. Our study uses fixed capacitors and switched capacitors to achieve the best possible solutions.

4.2 Problem Formulation:

The optimal capacitor placement problem in radial distribution systems, formulated as the following objective function, aims to minimize the total energy cost while maximizing savings:

$$\min S = K_P P_{\text{Total Loss}} + K_C Q_{\text{Total C}} = K_P \sum_{i=1}^{N_b-1} P_{\text{Loss}_i} + K_C \sum_{j=1}^{N_C} Q_{C_j} \qquad (4.1)$$

where:

- S: the total cost ($/year).
- K_P: the annual cost per unit of power loss ($/kW-year).
- K_C: the total capacitor purchase and installation cost ($/kVAR).
- $P_{\text{Total Loss}}$ and $Q_{\text{Total C}}$: the total power loss and total capacitive reactive power, respectively.
- P_{Loss_i}: the power loss in line i.
- Q_{C_j}: the total reactive power injected at location j.
- N_b: the total number of buses.
- N_C: the optimal number of capacitor placements.

We should note that K_P is taken equal to 168 $/(kW-year) while K_C is equal to 5 $/(kVAR).

The annual total cost of capacitors can be calculated as:

$$\text{Total capacitors cost} = \frac{K_C \times Q_{\text{Total C}}}{\text{Life expectancy}} \quad \$/\text{year} \qquad (4.2)$$

In this study the capacitors life expectancy is 10 years.

4.3 Operational Constraints:

The objective function (1) is subject to the following constraints:

a) Bus Voltage Constraint:

The voltage at each bus $\boldsymbol{V_i}$ must remain within its specified minimum and maximum limits:

$$V_{\min_i} \leq V_i \leq V_{\max_i} \qquad (4.3)$$

b) Capacitor Size Constraint:

The reactive power injection at each location must be within its feasible minimum and maximum limits:

$$Q_C^{\min_j} \leq Q_{C_j} \leq Q_C^{\max_j} \qquad (4.4)$$

where Q_{C_j} is the reactive power injection at location j.

c) Total Reactive Power Constraint:

The total reactive power injection ($\boldsymbol{Q}_{\text{Total C}}$) must be less than or equal to the total load reactive power ($\boldsymbol{Q}_{\text{Total L}}$):

$$Q_{\text{Total C}} \leq Q_{\text{Total L}} \qquad (4.5)$$

4.4 Ranking of Load Buses Based on Loss Sensitivity Indices (LSI1 and LSI2):

To reduce the computational complexity of the optimization process, the Loss Sensitivity Indices (LSI1 and LSI2) are first employed to evaluate the sensitivity of each load bus to power losses in the IEEE 34-bus distribution test system. Buses are then ranked in descending order of sensitivity to identify the most effective locations for capacitor placement. This pre-selection of candidate buses—prior to the application of the HHO and PSO optimization algorithms—ensures that both methods operate on a consistent and reduced search space, enabling a fair and efficient comparison of their performance in minimizing power losses and improving voltage profiles.

Rank	LSI1 Value	Bus Number (LSI1)	LSI2 Value	Bus Number (LSI2)
1	-1.1564e-5	11	9.9918e-6	11
2	-2.6370e-6	18	1.4980e-6	27
3	-2.5741e-6	24	1.2928e-6	18
4	-2.0374e-6	27	1.2007e-6	24
5	-1.9228e-6	4	6.3625e-7	9
6	-1.9099e-6	9	4.8931e-7	5
7	-1.8999e-6	5	4.8703e-7	2
8	-1.8444e-6	2	4.8337e-7	4
9	-1.8092e-6	19	4.7228e-7	25
10	-1.8065e-6	22	4.7209e-7	26
11	-1.8040e-6	23	4.7131e-7	23
12	-1.7987e-6	17	4.7042e-7	22
13	-1.7976e-6	25	4.6929e-7	19
14	-1.7959e-6	20	4.6907e-7	21
15	-1.7935e-6	26	4.6868e-7	20
16	-1.7923e-6	21	4.6867e-7	17
17	-1.7092e-6	8	4.5486e-7	8
18	-5.9895e-7	12	1.5820e-7	12
19	-1.8155e-7	28	5.1193e-8	29
20	-1.8147e-7	29	5.1192e-8	30
21	-1.8141e-7	30	5.1189e-8	28
22	-1.5574e-7	14	4.3289e-8	14
23	-1.5572e-7	13	4.3279e-8	15
24	-1.5560e-7	15	4.3274e-8	13
25	-1.0322e-7	32	2.6717e-8	32
26	-1.0319e-7	31	2.6713e-8	33
27	-1.0313e-7	33	2.6711e-8	34

Rank	LSI1 Value	Bus Number (LSI1)	LSI2 Value	Bus Number (LSI2)
28	-1.0309e-7	34	2.6705e-8	31
29	-8.6641e-9	3	1.2370e-9	3
30	-8.3389e-9	6	5.8184e-10	6
31	-5.1469e-9	16	1.2021e-9	16
32	-5.5342e-10	7	1.5414e-11	7
33	-2.5031e-11	10	6.9382e-13	10

Table 4.1: *LSI1 and LSI2 ranking for capacitor placement (input to HHO)*

Rank	LSI1 Value	Bus Number (LSI1)	LSI2 Value	Bus Number (LSI2)
1	-1.5328e-5	27	1.4124e-05	27
2	-7.9273e-6	21	6.3445e-06	2
3	-1.9428e-6	4	4.9061e-07	2
4	-1.9066e-6	5	4.8629e-07	4
5	-1.8628e-6	2	4.8225e-07	5
6	-1.8113e-6	24	4.7296e-07	24
7	-1.8093e-6	19	4.7255e-07	25
8	-1.8067e-6	22	4.7227e-07	26
9	-1.8051e-6	23	4.7140e-07	23
10	-1.8021e-6	17	4.7045e-07	22
11	-1.8020e-6	25	4.6952e-07	19
12	-1.7996e-6	20	4.6938e-07	17
13	-1.7973e-6	26	4.6924e-07	20
14	-1.7893e-6	18	4.6817e-07	18
15	-1.7350e-6	9	4.5929e-07	9
16	-1.7150e-6	11	4.5819e-07	11
17	-1.3453e-6	8	1.5919e-07	12
18	-6.0455e-7	12	9.4366e-08	8

Rank	LSI1 Value	Bus Number (LSI1)	LSI2 Value	Bus Number (LSI2)
19	-1.8255e-7	28	5.1381e-08	29
20	-1.8247e-7	29	5.1381e-08	30
21	-1.8241e-7	30	5.1378e-08	28
22	-1.5602e-7	14	4.3342e-08	14
23	-1.5600e-7	13	4.3332e-08	15
24	-1.5588e-7	15	4.3327e-08	13
25	-1.0413e-7	32	2.6875e-08	32
26	-1.0410e-7	31	2.6871e-08	33
27	-1.0404e-7	33	2.6869e-08	34
28	-1.0400e-7	34	2.6863e-08	31
29	-9.5797e-9	3	1.3669e-09	3
30	-8.8161e-9	6	1.2036e-09	16
31	-5.1562e-9	16	6.1428e-10	6
32	-7.1992e-10	7	2.0014e-11	7
33	-1.9814e-11	10	5.4762e-13	10

Table 4.2: *LSI1 and LSI2 ranking for capacitor placement (input to SPO)*

a) Discussion of LSIs ranking results:

- Buses such as 2, 4, 5, 24, and 27 consistently rank at the top of both LSI1 and LSI2, indicating high sensitivity to power losses and strong suitability for capacitor placement in the pre-optimization phase.
- In contrast, buses like 3, 6, 7, 10, and 16 are consistently ranked among the least sensitive, suggesting minimal impact on loss reduction and making them less favorable for reactive power compensation.
- The strong agreement between LSI1 and LSI2 rankings—both in top and bottom candidates—demonstrates a reliable correlation between these indices and the buses' effectiveness in reducing power losses, supporting their use for informed pre-selection.

- Although the optimization algorithms (HHO and PSO) differ in methodology, the same pre-selected set of buses is used for both, ensuring fairness and consistency in performance comparison.

Note: The rankings based on LSI1 and LSI2 are calculated independently of the optimization methods. Their sole purpose is to guide the optimization process by narrowing the search space to the most promising candidate buses.

To ensure equal opportunities for both fixed and switched capacitors in terms of optimal location and sizing, the candidate buses selected based on LSI1 and LSI2 (Tables 3.1 and 3.2) are unified. Accordingly, approximately 50% to 55% of the total buses (i.e., the top 17) are selected as control variables and passed into the optimization algorithms (HHO and PSO) for further processing.

$$C = \{x : x \in A \cap B\} \qquad (4.6)$$

where:

- C is the control variable set,
- A is the set of candidate buses based on LSI1,
- B is the set of candidate buses based on LSI2.

4.5 Application 1: Harris Hawks Optimization (HHO):

After selecting the most suitable candidate buses for capacitor placement based on Loss Sensitivity Indices (LSI1 and LSI2), the optimization of capacitor sizing and placement is carried out using Harris Hawks Optimization (HHO) first and then Particle Swarm Optimization (PSO) to compare their results.

To evaluate and compare the performance of HHO and PSO, three scenarios are analyzed for each algorithm:

- Base Case (Uncompensated System)

The original IEEE 34-bus radial distribution network is analyzed without any capacitor placement, serving as a benchmark. Key performance metrics include voltage magnitude (pu), total active power losses (kW), and total annual cost ($).

- Case 1 (Switched Capacitor Compensation)

Switched capacitors are installed at the pre-selected candidate buses.

Capacitor sizes are continuously adjustable within the range of 0 to 1200 kVAR, allowing for flexible reactive power compensation.

- Case 2 (Fixed Capacitor Compensation)

Capacitor sizes are constrained to discrete steps (multiples of 150 kVAR), from 0 to 1200 kVAR, reflecting a practical fixed-step installation approach.

Each case is evaluated in terms of voltage profile improvement, active power loss reduction, and cost minimization. This comparative study highlights the relative effectiveness of HHO and PSO in optimizing capacitor placement and sizing, offering insights into their performance and practical applicability in distribution network optimization.

The following flowchart presents the complete methodology used for optimal capacitor placement using the Harris Hawks Optimization (HHO) algorithm:

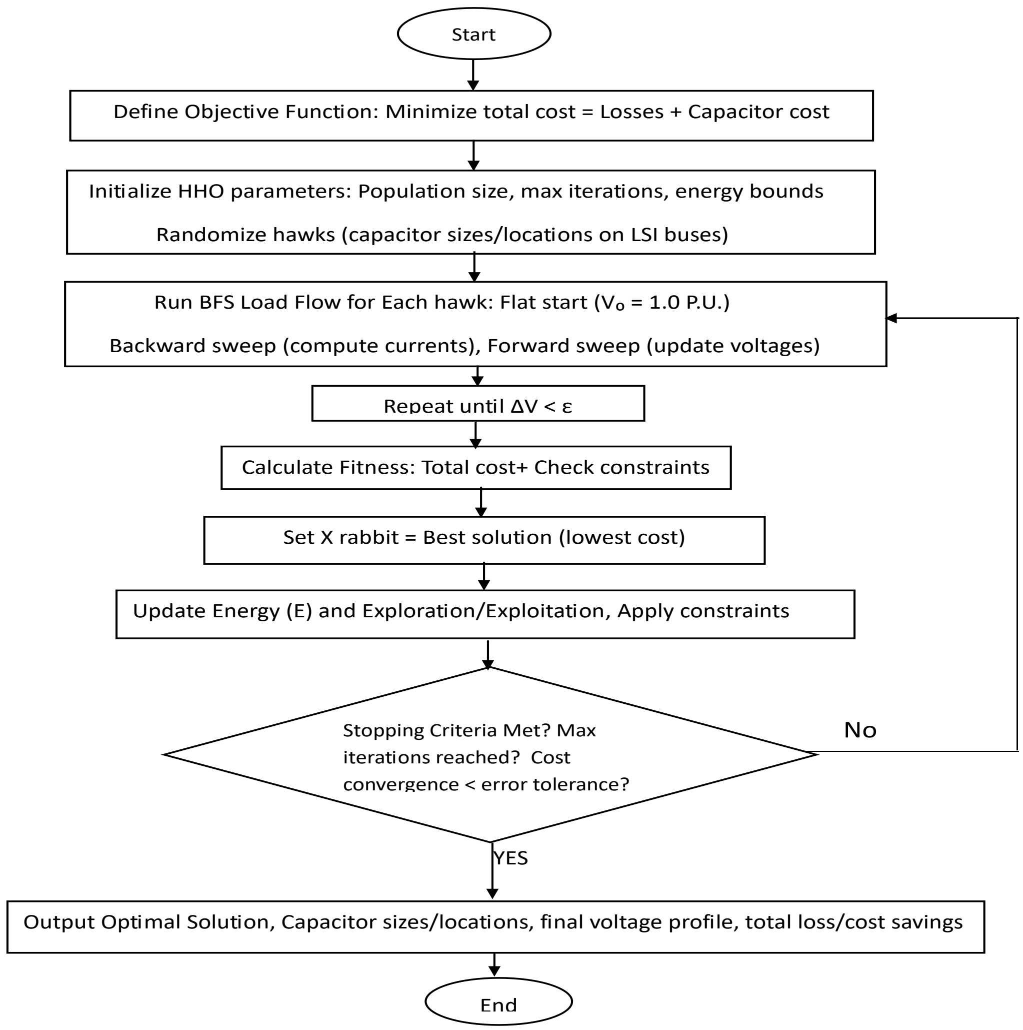

Figure 4.1: *Flow chart of optimization process via HHO*

a) Discussion of voltage profile (HHO):

The voltage profile comparison in Figure 4.2 demonstrates the effectiveness of capacitor placement optimization using the Harris Hawks Optimization (HHO) algorithm. The blue dashed line represents the uncompensated case, where the voltage magnitudes are significantly lower across all buses, highlighting weak voltage regulation and stability. In contrast, the red (Case 1) and black (Case 2) lines show considerable improvements in voltage stability after the optimal capacitor placement by the HHO algorithm.

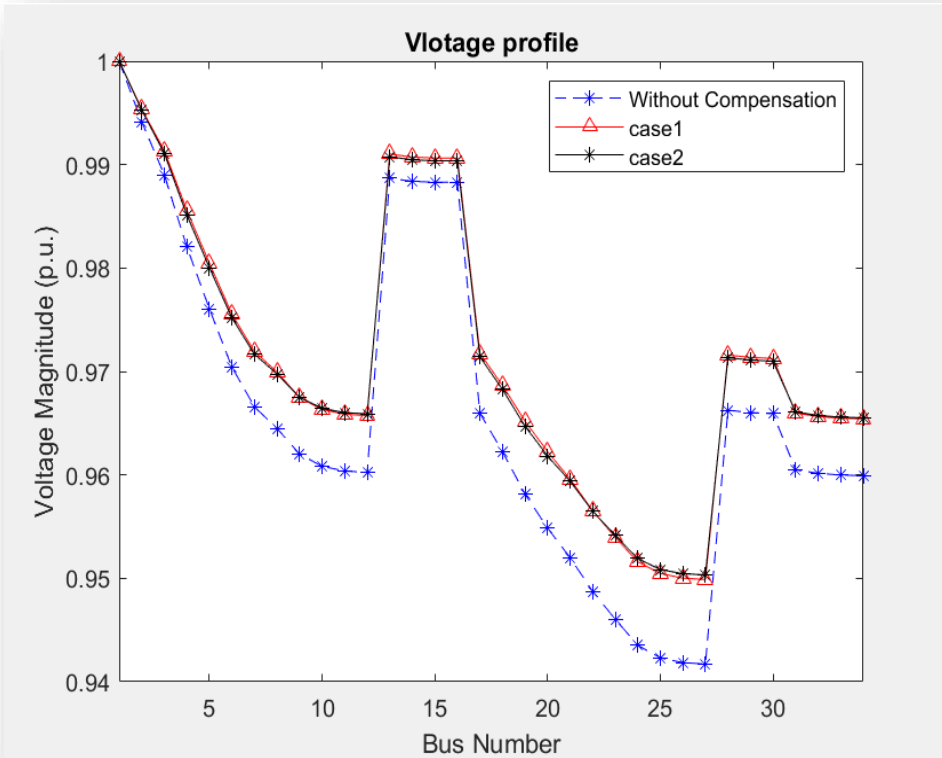

Figure 4.2: *Voltage Profile for Base, Switched, and Fixed Capacitor Cases (HHO)*

- Bus 2 has the highest voltage magnitude in all cases:
- Uncompensated case: 0.99414 pu.
- Case 1 (Switched capacitors): 0.99535 pu.
- Case 2 (Fixed capacitors): 0.99551 pu.

This indicates that Bus 2 experiences the least voltage drop and remains relatively stable in all cases. The slight increase in voltage magnitude in the compensated cases highlights the effectiveness of the HHO-based capacitor placement in maintaining a strong voltage profile at this bus.

- Bus 27 has the lowest voltage magnitude in all cases:

- Uncompensated case: 0.94171 pu.
- Case 1 (Switched capacitors): 0.9493 pu.
- Case 2 (Six capacitors): 0.95005 pu.

The voltage at Bus 27 is the most affected by drops due to its network position and reactive power demands. However, after applying Harris Hawks Optimization, the voltage at this bus improved significantly, particularly in Case 2, where it reached 0.95005 pu, ensuring better voltage stability at the weakest bus in the system.

➢ Overall Voltage Profile Improvement:

The voltage profile across the system has improved in both compensation cases. The increase in minimum voltage from 0.94171 pu (uncompensated) to 0.95005 pu (Case 2) at bus 27 demonstrates that the Harris Hawks Optimization for capacitor placement enhances voltage stability and controls excessive voltage drops, especially at the weakest buses. The maximum voltage also sees a minor improvement, ensuring that overcompensation is avoided while still enhancing system performance.

b) Discussion of Total Active Loss and Total Annual Cost (HHO):

Parameter	**Value**
Total Active Loss (kW)	221.7199
Total Annual Cost ($)	37248.9438
Minimum Voltage (pu)	0.94171 (Bus 27)
Maximum Voltage (pu)	0.99414 (Bus 2)

Table 4.3: *Parameters of the uncompensated network (HHO)*

Bus Number	**Capacitor Size (kVAR)**
5	298.02
24	370.52
18	384.96
9	311.71
11	810.28

Bus Number	**Capacitor Size (kVAR)**
7	338.89

***Table 4.4**: Capacitor placement and sizing in case 1 switched capacitors (HHO)*

Parameter	**Value**
Total Active Loss (kW)	162.59
Total Annual Cost ($)	27315.46
Minimum Voltage (pu)	0.9493 (Bus 27)
Maximum Voltage (pu)	0.99535 (Bus 2)
Total Capacitor Cost ($)	1257.19

***Table 4.5:** Parameters of the compensated network case 1 (HHO)*

Bus Number	Capacitor Size (kVAR)
18	300
9	600
5	150
2	450
19	300
20	450

***Table 4.6:** Capacitor placement and sizing in case 2 fixed capacitors (HHO)*

Parameter	Value
Total Active Loss (kW)	159.56
Total Annual Cost ($)	26807.40
Minimum Voltage (pu)	0.95005 (Bus 27)
Maximum Voltage (pu)	0.99551 (Bus 2)
Total Capacitor Cost ($)	1425

***Table 4.7**: Parameters of the compensated network case 2 (HHO)*

The results obtained using the Harris Hawks Optimization (HHO) algorithm demonstrate a clear improvement in system performance through optimized capacitor placement and sizing. Below are the key observations based on the analysis of the three studied cases:

- Base Case (Uncompensated System)

The system without any compensation experienced the highest total active power losses at 221.72 kW, with a corresponding total annual cost of $37,248.94. The minimum voltage was 0.94171 pu. (Bus 27), indicating the weakest voltage condition in the system.

- Case 1 – Compensation with Switched Capacitors

When continuously adjustable capacitors were placed at six selected buses, total active losses were reduced significantly to 162.59 kW, representing a 26.65% reduction compared to the base case. The total annual cost dropped to $27,315.46, and the voltage profile improved, with the minimum voltage rising to 0.9493 pu (Bus 27). Capacitor sizes varied between approximately 298 KVAR and 810 kVAR, and the total cost of capacitors was $1,257.19.

- Case 2 – Compensation with Fixed Capacitors

When capacitor sizes were restricted to discrete steps (multiples of 150 kVAR), the system achieved slightly better performance than in Case 1. The total active loss was further reduced to 159.56 kW, and the total annual cost decreased to $26,807.40. The minimum voltage improved to 0.95005 pu, and the total capacitor cost was $1,425, slightly higher than in Case 1 but with better performance.

4.6 Application 2: Particle Swarm Optimization (PSO):

The following flowchart presents the complete methodology used for optimal capacitor placement using the Particle Swarm Optimization (PSO) algorithm.

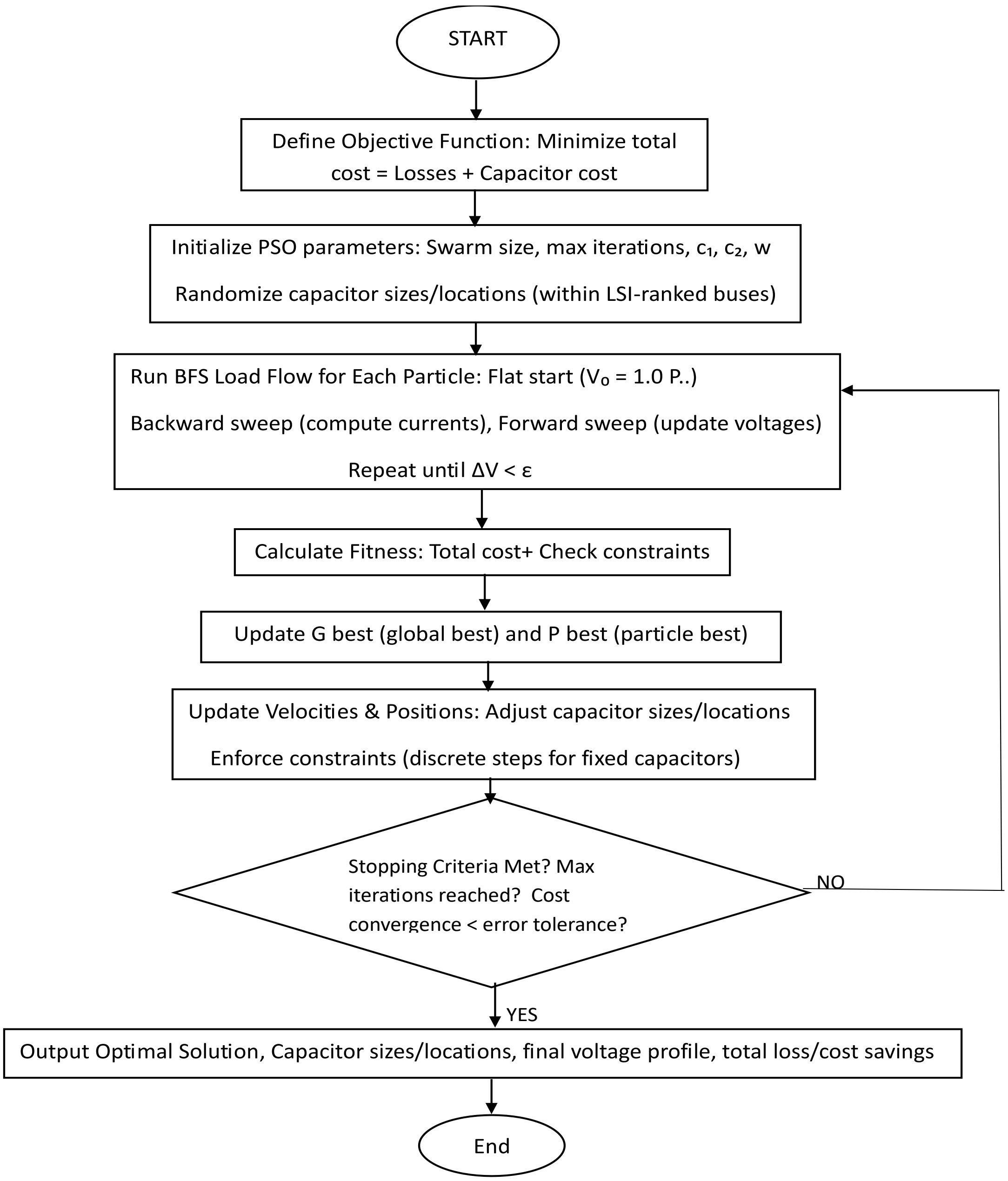

Figure 4.3: *Flow chart of optimization process via PSO*

a) Discussion of voltage profile (PSO):

Similar to the results obtained with the HHO algorithm, the voltage profile shown in Figure 4.4 demonstrates the impact of optimal capacitor placement using the Particle Swarm Optimization (PSO) algorithm. The uncompensated case, represented by the blue dashed line, shows lower voltage levels throughout the system, while the compensated cases (red for Case 1 and black for Case 2) clearly illustrate improved voltage stability and regulation as a result of the PSO-based optimization.

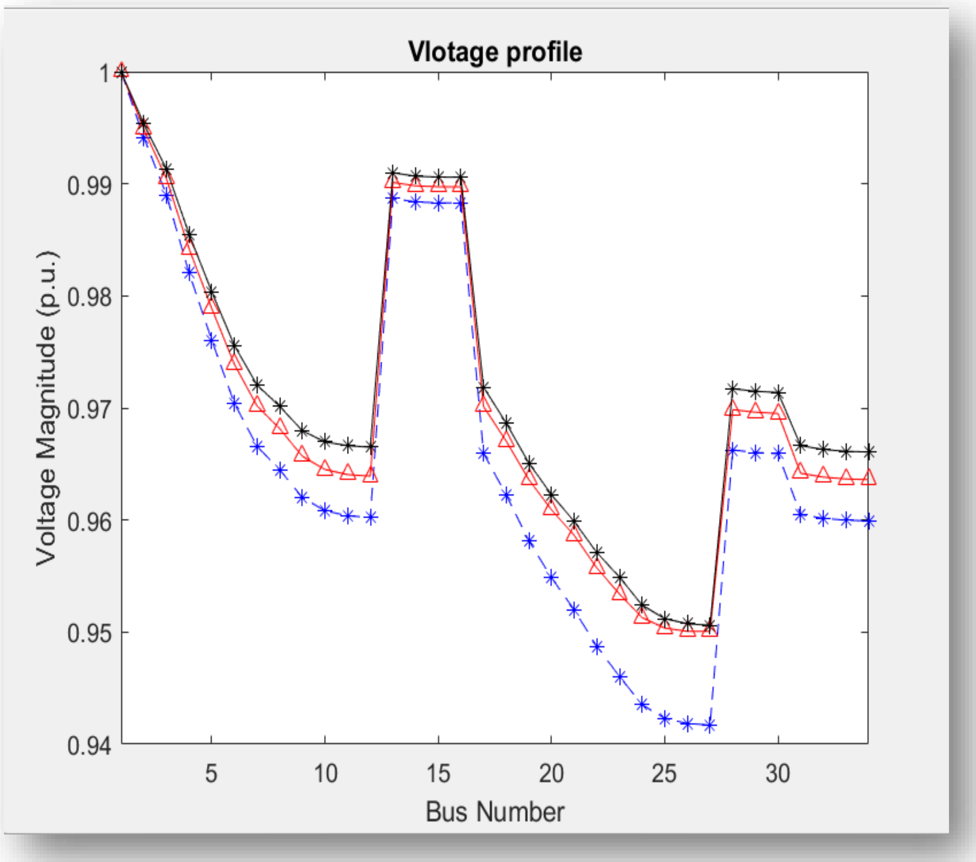

Figure 4.4: *Voltage Profile for Base, Switched, and Fixed Capacitor Case (PSO)*

➢ Uncompensated Case:

The voltage at Bus 27 dropped to 0.941713 pu, indicating a weak voltage profile at the far end of the electrical network. Bus 2 maintained a relatively high voltage at 0.994137 pu, but overall voltage regulation was poor.

➢ Case 1 – Switched Capacitors:

After PSO-optimized placement of switched capacitors, the voltage at Bus 27 improved to 0.950070 pu, and Bus 2 rose slightly to 0.994886 pu. This shows that switched capacitors provided dynamic support and improved the overall voltage profile effectively.

➢ Case 2 – Fixed Capacitors:

Fixed capacitors resulted in the best voltage performance, with Bus 27 reaching 0.950610 pu and Bus 2 increasing to 0.995335 pu. This shows that fixed capacitors provided slightly more effective at voltage profile enhancement.

Both compensated cases achieved voltage levels well within acceptable regulatory limits (typically 0.95–1.05 pu), thus contributing to better power quality and network reliability.

b) Discussion of Total Active Loss and Total Annual Cost (PSO):

Parameter	**Value**
Total Active Loss (kW)	221.7199
Total Annual Cost ($)	37248.9438
Minimum Voltage (pu)	0.94171 (Bus 27)
Maximum Voltage (pu)	0.99414 (Bus 2)

Table 4.8: *Parameters of the uncompensated network (PSO)*

Bus Number	**Capacitor Size (kVAR)**
22	214.39
21	430.29
26	830.73
11	335.38

***Table 4.9**: Capacitor placement and sizing in case 1 switched capacitors (PSO)*

Parameter	**Value**
Total Active Loss (kW)	165.57
Total Annual Cost ($)	27817.33
Minimum Voltage (pu)	0.95007 (Bus 27)
Maximum Voltage (pu)	0.99488 (Bus 2)
Total Capacitor Cost ($)	905.40

***Table 4.10:** Parameters of the compensated network case 1 (PSO)*

Bus Number	Capacitor Size (kVAR)
4	600
24	750
20	600
8	900

***Table 4.11:** Capacitor placement and sizing in case 2 fixed capacitors (PSO)*

Parameter	Value
Total Active Loss (kW)	160.24
Total Annual Cost ($)	26920.98
Minimum Voltage (pu)	0.950610 (Bus 27)
Maximum Voltage (pu)	0.995335 (Bus 2)
Total Capacitor Cost ($)	1425

***Table 4.12:** Parameters of the compensated network case 2 (PSO)*

- The PSO algorithm effectively reduced total active power loss from 221.72 kW in the uncompensated system to 165.57 kW in Case 1 (switched capacitors) and further to 160.24 kW in Case 2 (fixed capacitors).
- Correspondingly, the total annual cost dropped significantly from $37,248.94 to $27,817.33 in Case 1 and $26,920.98 in Case 2, indicating a clear economic advantage of optimized compensation.
- In Case 1, PSO selected fewer buses (only 4) with continuously adjustable capacitor sizes, demonstrating its capability to minimize investment while achieving noticeable improvement.
- Case 2 involved fixed-size capacitors at different buses with higher total capacitor costs ($1,425), but still achieved better loss reduction, suggesting that discrete capacitor placement can be more effective in certain configurations.

4.7 Comparative Analysis between PSO and HHO:

Both PSO and HHO algorithms significantly improved the performance of the radial distribution network in terms of power loss reduction, voltage profile enhancement, and cost minimization. However, there are differences in their optimization strategies, particularly regarding capacitor placement.

- Number and Distribution of Capacitors:

One of the most striking differences between the two methods is the number of capacitor placements.

- PSO selected 4 capacitor locations in both Case 1 (switched) and Case 2 (fixed).
- HHO, on the other hand, opted for 6 capacitor placements in each case.

This broader distribution by HHO allowed for a more granular compensation across the network, which contributed to slightly better power loss reduction and voltage stability, especially in Case 2. By dispersing reactive power support over a greater number of buses, HHO provided a more balanced voltage profile and more effective mitigation of line losses.

- Power Loss Reduction:

- PSO Case 2 (Fixed): Reduced losses from 221.72 kW to 160.24 kW.
- HHO Case 2 (Fixed): Reduced losses to 159.56 kW, which is marginally better.

This small improvement reflects the effectiveness of HHO's wider capacitor placement in addressing reactive power demands more precisely.

- Total Annual Cost:

- PSO Case 2: Final cost was $26,920.98.
- HHO Case 2: Slightly better at $26,807.40, despite placing more capacitors.

This implies that HHO’s optimized placement strategy justifies the use of more capacitors by achieving superior technical performance without incurring significantly higher capital costs.

- Capacitor Cost:

Interestingly, the total capacitor cost in Case 2 was identical for both algorithms at $1425, which further validates HHO’s efficiency. Even with two additional capacitors, the algorithm maintained the cost within the same limit by selecting smaller-sized capacitors, thus spreading the compensation effort economically and efficiently.

- Minimum Bus Voltage:

Both algorithms achieved similar improvements in minimum voltage, raising it to around 0.9500 pu, compared to 0.94171 pu in the uncompensated case.

Overall, both PSO and HHO are effective for capacitor placement optimization, but HHO demonstrates a more refined and systematic approach by using a higher number of capacitors with optimized sizing and strategic placement, leading to better performance metrics without increasing total cost. This makes HHO more suitable for systems where fine-tuned compensation and long-term loss reduction are priorities.

Category	Metric	Uncompensated	PSO – Case 1 (Switched capacitors)	PSO – Case 2 (Fixed capacitors)	HHO – Case 1 (Switched)	HHO – Case 2 (Fixed)
Total Active Loss (kW)	–	221.72	165.57	160.24	162.59	159.56
Total Annual Cost ($)	–	37248.94	27817.33	26920.98	27315.46	26807.40
Minimum Voltage (pu)	(Bus 27)	0.94171	0.95007	0.95061	0.9493	0.95005
Maximum Voltage (pu)	(Bus 2)	0.99414	0.99488	0.99534	0.99535	0.99551
Capacitor Cost ($)	–	–	905.40	1425	1257.19	1425
No. of Capacitor Buses	–	–	4	4	6	6
Capacitor Sizing (kVAR)	–	–	[214.39, 430.29, 830.73, 335.38]	[600, 750, 600, 900]	[298.02, 370.52, 384.96, 311.71, 810.28, 338.89]	[300, 600, 150, 450, 300, 450]

***Table 4.13**: Performance Comparison between PSO and HHO*

As shown in Table 4.13, both PSO and HHO achieved significant improvements in power loss reduction, voltage regulation, and cost savings compared to the uncompensated case. However, HHO consistently demonstrated slightly better performance in all key metrics, particularly in power loss reduction and overall cost efficiency, without incurring higher capacitor costs. These results confirm the effectiveness of HHO's strategy of distributing smaller capacitors across more buses, thereby enhancing network compensation while maintaining economic feasibility.

4.8 Conclusion:

This chapter presents the results of our two-stage approach—combining Loss Sensitivity Indices (LSIs) with HHO and PSO algorithms—for optimal capacitor placement in radial distribution systems. Both algorithms significantly reduced power losses, improved voltage profiles, and minimized costs, with HHO showing marginally better performance due to its strategic capacitor distribution. The results validate the practicality of metaheuristic optimization in enhancing distribution network efficiency while meeting operational constraints.

General Conclusion

This thesis presented a robust and efficient two-stage optimization approach for optimal capacitor placement in Radial Distribution Networks (RDNs), aimed at minimizing power losses, improving voltage profiles, and reducing total operational costs. The methodology combined Loss Sensitivity Indices (LSIs) with advanced metaheuristic algorithms — specifically Particle Swarm Optimization (PSO) and Harris Hawks Optimization (HHO) — to achieve a well-balanced solution strategy.

The first stage, based on LSIs, provided a fast analytical means of identifying buses that were most sensitive to power losses. However, LSIs alone were insufficient due to their static nature: once sensitive buses are identified, they remain fixed, which restricts the solution space and limits the potential for more optimal capacitor configurations. In contrast, using only metaheuristic algorithms without prior bus filtering would have significantly increased the computational complexity and search time. The two-stage approach addressed both concerns — using LSIs to narrow the candidate locations and metaheuristics to dynamically search and optimize within that refined space. This approach combined analytical efficiency with algorithmic flexibility.

Simulation results on the IEEE 34-bus test system demonstrated that this hybrid methodology yielded significant performance improvements. Among the tested algorithms, HHO consistently outperformed PSO in terms of power loss reduction, voltage profile enhancement, and cost minimization. HHO's success is attributed to its stronger balance between exploration and exploitation capabilities, which allowed it to avoid premature convergence and escape local optima, leading to more globally efficient solutions.

These findings confirm the added value of integrating analytical techniques with intelligent optimization in distribution network planning. The proposed framework is not only effective but also scalable and adaptable to evolving grid conditions. It reflects an important shift toward smarter and more resilient power systems capable of meeting modern operational challenges.

Looking forward, the methodology could be extended to consider dynamic load variations, real-time control strategies, and the integration of distributed renewable energy sources. These enhancements would further strengthen the practical utility and responsiveness of the system under real-world operating conditions.

In conclusion, this research provides a significant contribution to the field of distribution network optimization by demonstrating the advantages of a hybrid LSIs–metaheuristic approach. The superior performance of HHO reinforces its potential as a powerful tool in future power system applications, particularly in smart grid and energy management contexts.

Annex

Sending bus	Receiving bus	R(ohm)	X(ohm)	Line numbers
1	2	0.117	0.048	1
2	3	0.10725	0.044	2
3	4	0.16445	0.04565	3
4	5	0.1495	0.0415	4
5	6	0.1495	0.0415	5
6	7	0.3144	0.054	6
7	8	0.2096	0.036	7
8	9	0.3144	0.054	8
9	10	0.2096	0.036	9
10	11	0.131	0.0225	10
11	12	0.1048	0.018	11
3	13	0.1572	0.027	12
13	14	0.2096	0.036	13
14	15	0.1048	0.018	14
15	16	0.0524	0.009	15
6	17	0.1794	0.0498	16
17	18	0.16445	0.04565	17
18	19	0.2079	0.0473	18
19	20	0.189	0.043	19
20	21	0.189	0.043	20
21	22	0.262	0.045	21
22	23	0.262	0.045	22
23	24	0.3144	0.054	23
24	25	0.2096	0.036	24
25	26	0.131	0.0225	25
26	27	0.1048	0.018	26
7	28	0.1572	0.027	27
28	29	0.1572	0.027	28
29	30	0.1572	0.027	29
10	31	0.1572	0.027	30
31	32	0.2096	0.036	31
32	33	0.1072	0.027	32
33	34	0.1048	0.018	33

Table A.1:*Distribution Network Line Data*

Bus number	P(kW)	Q(kVAR)
1	0	0
2	230	142.5
3	0	0
4	230	142.5
5	230	142.5
6	0	0
7	0	0
8	230	142.5
9	230	142.5
10	0	84
11	230	45
12	137	45
13	72	45
14	72	7.5
15	72	142.5
16	13.5	142.5
17	230	142.5
18	230	142.5
19	230	142.5
20	230	142.5
21	230	142.5
22	230	142.5
23	230	142.5
24	230	142.5
25	230	142.5
26	230	142.5
27	137	85
28	75	48
29	75	48
30	75	48
31	57	34.5
32	57	34.5
33	57	34.5
34	57	34.5

Table A.2*:Load Data for Each Bus*

References

[1] Narimen AOUZELLAG. « Contribution à l'Amélioration de la Flexibilité dans les Réseaux Electriques liée à l'Intégration des Générateurs Eoliens » Thèse Doctorat. 2011

[2] J. D. Glover, M. S. Sarma, and T. J. Overbye, *Power System Analysis and Design*, 6th ed., Boston, MA, USA: Cengage Learning, 2017.

[3] F. Karbalaei, S. Abbasi, and H. R. Shabani, "Generator modeling," in *Voltage Stability in Electrical Power Systems: Concepts, Assessment, and Methods for Improvement*, IEEE, 2023, pp. 47–82.

[4] H. Saadat, *Power System Analysis*, 2nd ed., New York, NY, USA: McGraw-Hill, 2002.

[5] C. Christopoulos and A. Wright, *Electrical Power System Protection*. Springer, 2013.

[6] A. Y. Abdelaziz, S. H. E. Abdel Aleem, and A. Yadav, Eds., *Artificial Intelligence Applications in Electrical Transmission and Distribution Systems Protection*. Boca Raton, FL, USA: CRC Press, 2021

[7] R. Parasher, "Load flow analysis of radial distribution network using linear data structure

[8] W.D. Stevenson, "Elements of Power System Analysis", 4th Ed., McGraw-Hill Book 1982.

[9] Z. Wang, "*Power flow in distribution systems*," Iowa State University, Ames, IA, USA.

[10] A. A. Abou El-Ela, R. A. El-Sehiemy, A.-M. Kinawy, and M. T. Mouwafi, "Optimal capacitor placement in distribution systems for power loss reduction and voltage profile improvement," *IET Generation, Transmission & Distribution*, vol. 10, no. 5, pp. 1209–1221, 2016.

[11] M. Abujubbeh and B. Natarajan, "Overview of Loss Sensitivity Analysis in Modern Distribution Systems," *IEEE Access*, vol. 10, pp. 16037–16049, 2022.

[12] B. Jangid and S. Ghosh, "Load Flow Analysis using Backward Forward Sweep Method," in *Proc. Int. Conf. Advancements in Engineering and Technology (ICAET)*, 2017, pp. 9–10.

[13] G. A. Setia, G. H. M. Sianipar, K. Samudra, F. Haz, N. Winanti, and H. R. Iskandar, "Implementation of Backward-Forward Sweep Method on Load Model Variation of Distribution Systems," in *Proc. 2019 2nd Int. Conf. on High Voltage Engineering and Power Systems (ICHVEPS)*, Denpasar, Indonesia, 2019, pp. 1–5.

[14] M. Gendreau and J.-Y. Potvin, Eds., *Handbook of Metaheuristics*, 3rd ed. Cham, Switzerland: Springer, 2019.

References

[15] A. H. Gandomi, X.-S. Yang, S. Talatahari, and A. H. Alavi, "Metaheuristic algorithms," in *Metaheuristic Applications in Structures and Infrastructures*, Waltham, MA, USA: Elsevier, 2013, pp. 1–24.

[16] J. Shi and Q. Zhang, “A new cooperative framework for parallel trajectory-based metaheuristics,” *Applied Soft Computing*, vol. 65, pp. 374–386, 2018.

[17] L. Brezočnik, I. Fister Jr., and V. Podgorelec, “Swarm intelligence algorithms for feature selection: A review,” *Applied Sciences*, vol. 8, no. 9, p. 1521, 2018.

[18] A. A. Heidari, S. Mirjalili, H. Faris, I. Aljarah, M. Mafarja, and H. Chen, "Harris hawks optimization: Algorithm and applications," *Future Generation Computer Systems*, vol. 97, pp. 849–872, Aug. 2019.

[19] S. Sengupta, S. Basak, and R. A. Peters II, "Particle Swarm Optimization: A survey of historical and recent developments with hybridization perspectives," *Machine Learning and Knowledge Extraction*, vol. 1, no. 1, pp. 157–191, 2019.

[20] J. Kennedy and R. Eberhart, "Particle swarm optimization," Proceedings of ICNN'95 - International Conference on Neural Networks, Perth, WA, Australia, 1995, pp. 1942-1948 vol.4.

[21] M. Pant, “Particle Swarm Optimization, Department of Applied Science and Engineering,” Saharanpur Campus of IIT Roorkee. 2009.

[22] H. M. Alabool, D. Alarabiat, L. Abualigah, and A. A. Heidari, “Harris hawks’ optimization: A comprehensive review of recent variants and applications,” *Neural Comput. Appl.*, vol. 33, pp. 8939–8980, 2021